

Giant Tree Frog diversification in West and Central Africa: Isolation by physical barriers, climate, and reproductive traits

Kyle E. Jaynes^{1,2,3,4}  | Edward A. Myers²  | Václav Gvoždík^{5,6}  |
 David C. Blackburn⁷  | Daniel M. Portik⁸  | Eli Greenbaum⁹  |
 Gregory F. M. Jongsma^{7,10}  | Mark-Oliver Rödel¹¹ | Gabriel Badjedjea¹² |
 Abraham Bamba-Kaya¹³ | Ninda L. Baptista^{14,15,16} | Jeannot B. Akuboy¹⁷ |
 Raffael Ernst¹⁸  | Marcel T. Kouete^{7,19} | Chifundera Kusamba²⁰ | Franck M. Masudi¹⁷  |
 Patrick J. McLaughlin^{21,22}  | Lotanna M. Nneji²³  | Abiodun B. Onadeko²⁴  |
 Johannes Penner^{11,25}  | Pedro Vaz Pinto^{14,26}  | Bryan L. Stuart²⁷  | Elie Tobi²⁸ |
 Ange-Ghislain Zassi-Boulou²⁹ | Adam D. Leaché³⁰  | Matthew K. Fujita³¹  |
 Rayna C. Bell^{2,8} 

¹Department of Biology, Adrian College, Michigan, USA

²Department of Vertebrate Zoology, National Museum of Natural History, Smithsonian Institution, Washington, DC, USA

³Department of Integrative Biology, W.K. Kellogg Biological Station, Michigan State University, Michigan, USA

⁴Ecology, Evolution, and Behavior Program, Michigan State University, Michigan, USA

⁵Institute of Vertebrate Biology, Czech Academy of Sciences, Brno, Czech Republic

⁶Department of Zoology, National Museum, Prague, Czech Republic

⁷Department of Natural History, Florida Museum of Natural History, University of Florida, Gainesville, Florida, USA

⁸Herpetology Department, Institute for Biodiversity Science and Sustainability, California Academy of Sciences, San Francisco, California, USA

⁹Department of Biological Sciences, University of Texas at El Paso, El Paso, Texas, USA

¹⁰Department of Biology, University of Florida, Florida, USA

¹¹Leibniz Institute for Evolution and Biodiversity Science, Museum für Naturkunde, Berlin, Germany

¹²Département d'Ecologie et Biodiversité des Ressources Aquatiques, Centre de Surveillance de la Biodiversité, Université de Kisangani, Kisangani, République Démocratique du Congo

¹³Institute de Recherches Agronomiques et Forestières, Libreville, Gabon

¹⁴CIBIO/InBio – Centro de Investigação em Biodiversidade e Recursos Genéticos, Universidade do Porto, Campus de Vairão, Vairão, Portugal

¹⁵Faculdade de Ciências da, Universidade do Porto, Porto, Portugal

¹⁶Instituto Superior de Ciências da Educação da Huíla (ISCED-Huíla), Rua Sarmento Rodrigues, Lubango, Angola

¹⁷Département d'Ecologie et Biodiversité des Ressources Terrestres, Centre de Surveillance de la Biodiversité, Université de Kisangani, République Démocratique du Congo, Kisangani

¹⁸Museum of Zoology, Senckenberg Natural History Collections Dresden, Dresden, Germany

¹⁹School of Natural Resources and Environment, University of Florida, Florida, USA

²⁰Laboratoire d'Herpétologie, Département de Biologie, Centre de Recherche en Sciences Naturelles, République Démocratique du Congo, Lwiro

²¹Bioko Biodiversity Protection Project, Drexel University, Philadelphia, Pennsylvania, USA

²²Institute of Conservation Science and Learning, Bristol Zoological Society, Bristol, UK

²³Department of Ecology and Evolutionary Biology, Princeton University, New Jersey, USA

²⁴Department of Zoology, Faculty of Science, University of Lagos, Lagos, Nigeria

²⁵Chair of Wildlife Ecology and Wildlife Management, University of Freiburg, Freiburg, Germany

²⁶Fundação Kissama, Luanda, Angola

²⁷Section of Research & Collections, North Carolina Museum of Natural Sciences, North Carolina, USA

Kyle E. Jaynes and Edward A. Myers contributed equally.

²⁸Gabon Biodiversity Program, Smithsonian Conservation Biology Institute, Gamba, Gabon

²⁹Institut National de Recherche en Sciences Exactes et Naturelles, Brazzaville, République du Congo

³⁰Department of Biology & Burke Museum of Natural History and Culture, University of Washington, Seattle, Washington, USA

³¹Amphibian and Reptile Diversity Research Center, Department of Biology, University of Texas at Arlington, Arlington, Texas, USA

Correspondence

Kyle E. Jaynes, W.K. Kellogg Biological Station, Michigan State University, Michigan, USA.

Email: jaynesky@msu.edu

Edward A. Myers, Department of Biological Sciences, Clemson University, South Carolina, USA.

Email: eddie.a.myers@gmail.com

Rayna C. Bell, Herpetology Department, Institute for Biodiversity Science and Sustainability, California Academy of Sciences, California, USA.

Email: rbell@calacademy.org

Funding information

U.S. National Science Foundation, Grant/Award Number: DEB-1145459, DEB-1202609, DEB-1456098, DEB-1457232, EF-1241885 and OCE-1560088; Grantová Agentura České Republiky, Grant/Award Number: GACR15-13415Y; Natural Sciences and Engineering Research Council of Canada, Grant/Award Number: PGSD2/516563-2018; National Geographic Society, Grant/Award Number: 8556-08; Fundação para a Ciência e a Tecnologia, Grant/Award Number: SFRH/PD/BD/140810/2018 and UIDB/50027/2020

Abstract

Secondary sympatry amongst sister lineages is strongly associated with genetic and ecological divergence. This pattern suggests that for closely related species to coexist in secondary sympatry, they must accumulate differences in traits that mediate ecological and/or reproductive isolation. Here, we characterized inter- and intraspecific divergence in three giant tree frog species whose distributions stretch across West and Central Africa. Using genome-wide single-nucleotide polymorphism data, we demonstrated that species-level divergence coincides temporally and geographically with a period of large-scale forest fragmentation during the late Pliocene. Our environmental niche models further supported a dynamic history of climatic suitability and stability, and indicated that all three species occupy distinct environmental niches. We found modest morphological differentiation amongst the species with significant divergence in tympanum diameter and male advertisement call. In addition, we confirmed that two species occur in secondary sympatry in Central Africa but found no evidence of hybridization. These patterns support the hypothesis that cycles of genetic exchange and isolation across West and Central Africa have contributed to globally significant biodiversity. Furthermore, divergence in both ecology and reproductive traits appear to have played important roles in maintaining distinct lineages. At the intraspecific level, we found that climatic refugia, precipitation gradients, marine incursions, and potentially riverine barriers generated phylogeographic structure throughout the Pleistocene and into the Holocene. Further studies examining phenotypic divergence and secondary contact amongst these geographically structured populations may demonstrate how smaller scale and more recent biogeographic barriers contribute to regional diversification.

KEYWORDS

demographic modelling, divergence, ecological niche, land-bridge island, phylogeography, refugia

La sympatrie secondaire parmi les espèces sœurs est fortement associée à la divergence génétique et écologique. Ce modèle suggère que pour que des espèces étroitement liées coexistent en sympatrie secondaire, elles doivent accumuler des différences dans les traits qui contribuent à l'isolement écologique ou reproductif. Ici, nous avons caractérisé la divergence inter- et intra-spécifique chez trois espèces de grenouilles arboricoles géantes dont les distributions s'étendent à travers l'Afrique de l'Ouest et Centrale. Avec des données génétiques, nous avons démontré que la divergence au niveau des espèces coïncide temporellement et géographiquement avec une période de fragmentation forestière à la fin du Pliocène. Nos modèles de niches environnementales ont soutenu une histoire dynamique de stabilité climatique, et ont indiqué que les trois espèces occupent des niches environnementales distinctes. Nous avons trouvé une différenciation morphologique modeste parmi les trois espèces mais une divergence significative dans le diamètre du tympan et les cris des mâles. De plus, nous avons confirmé que deux espèces sont présentes en sympatrie secondaire

en Afrique Centrale mais n'avons trouvé aucune preuve d'hybridation. Ces résultats soutiennent l'hypothèse que les cycles d'échange génétique et d'isolement à travers l'Afrique de l'Ouest et Centrale ont contribué à une profonde concentration de biodiversité dans la région. De plus, la divergence des traits écologiques et reproducteurs semble avoir joué un rôle important dans le maintien de lignées distinctes. Au niveau intra-spécifique, nous avons constaté que les refuges climatiques, les gradients de précipitation, les incursions marines et potentiellement les barrières fluviales ont généré une structure phylogéographique pendant le Pléistocène et jusqu'à l'Holocène. Des études examinant la divergence phénotypique et le contact secondaire entre ces populations géographiquement structurées pourraient démontrer comment des barrières biogéographiques à échelle plus petite et plus récentes contribuent à la diversification régionale.

1 | INTRODUCTION

Speciation typically occurs when populations become isolated by a physical barrier such that gene flow between populations ceases (Fitzpatrick et al., 2009; Mayr, 1942). If these allopatric populations inhabit contrasting environments, then ecological and morphological differentiation may evolve due to local adaptation (Ryan et al., 2007; Schluter, 2009). Alternatively, allopatric lineages may exhibit ecological niche conservatism and remain morphologically similar, yet continue to diverge and ultimately speciate (Wiens, 2004). Secondary sympatry amongst congeneric species is strongly associated with genetic and morphological divergence, which suggests that for closely related species to coexist in secondary sympatry, they must differ in traits that mediate ecological and/or reproductive isolation (Friis & Milá, 2020; Krishnan & Tamma, 2016; Pigot & Tobias, 2015; Xu & Shaw, 2020). Quantifying divergence in ecological, morphological, and sexually selected traits amongst closely related lineages can provide insight into the processes that enable secondary sympatry and the accumulation of species richness.

Across West and Central Africa, a dynamic suite of landscape features and ecological gradients coincide with globally significant biodiversity (Couvreur et al., 2021; Myers et al., 2000). Time-calibrated phylogenies indicate that much of this diversity arose in situ during the late Miocene to mid Pleistocene (e.g. Koenen et al., 2015; Njabo et al., 2008; Portik et al., 2019; Springer et al., 2012; Tolley et al., 2013; reviewed in Couvreur et al., 2021). Prominent geographic features that may have played a role in generating this diversity include the Dahomey Gap, a dry savannah that bisects the West African rainforests (Booth, 1958; Salzmann & Hoelzmann, 2005), the mountains of the Cameroon Volcanic Line that extend into the Gulf of Guinea forming an archipelago of land-bridge and oceanic islands (Marzoli et al., 2000), and several large rivers (Goudie, 2005; Figure 1). This region is also characterized by precipitation gradients with extensive variation in both annual precipitation and seasonality that vary across longitude and latitude, resulting in a patchwork of vegetation types (Couvreur et al., 2021; Marshall et al.,

2021). Consequently, species diversification across this region is attributed to many geographic and ecological mechanisms including lowland forest or montane refugia, riverine barriers, marine incursions, and ecological gradients (Couvreur et al., 2021; Hardy et al., 2013; Penner et al., 2011). To date, empirical studies have primarily characterized patterns of phylogeographic structure within species with respect to these proposed biogeographic features. Thus, our understanding is still limited with respect to the geographic context of speciation, the extent of phenotypic and/or ecological divergence amongst sister lineages, and how these processes interact to result in secondary sympatry and exceptional regional species diversity.

Here we characterize genetic and phenotypic diversification in three closely related species of *Leptopelis* tree frogs whose distributions stretch across West (*L. macrotis*; Schiøtz, 1967) and Central (*L. millsoni*; [Boulenger, 1895], *L. rufus*; Reichenow, 1874) Africa (Figure 1; Jaynes et al., 2021). All three species are arboreal and amongst the largest in the genus, with females reaching up to 87 mm snout-vent length (Channing & Rödel, 2019; Schiøtz, 1999). These species occur both in allopatry and in broad parapatry, and collectively their distributions span all major physical barriers and ecological gradients across West and Central Africa including the land-bridge island Bioko and the 'climatic hinge', a north-to-south seasonal inversion at 0–3°N along the southern border of Cameroon (Hardy et al., 2013; Figure 1). Despite this vast distribution and the recognition of multiple distinct lineages (Jaynes et al., 2021; Portik et al., 2019), the species are remarkably challenging to identify based on morphology alone, which resulted in taxonomic confusion for over a century (Ahl, 1929, 1931; Noble, 1924; Perret, 1973; Schiøtz, 1967). As a legacy of this confusion, the extent to which *L. rufus* and *L. millsoni* occur in true sympatry (i.e. syntopy) in western Central Africa is unclear. Furthermore, *L. macrotis* has been considered a subspecies of *L. millsoni* by some authors (Amiet, 2012) and the geographic boundary between *L. macrotis* and *L. millsoni* in West Africa remains uncertain (Rödel et al., 2014). More recently, the three species have been proposed to differ in tympanum size (Amiet, 2012; Schiøtz, 1999), which likely has functional consequences for auditory sensitivity

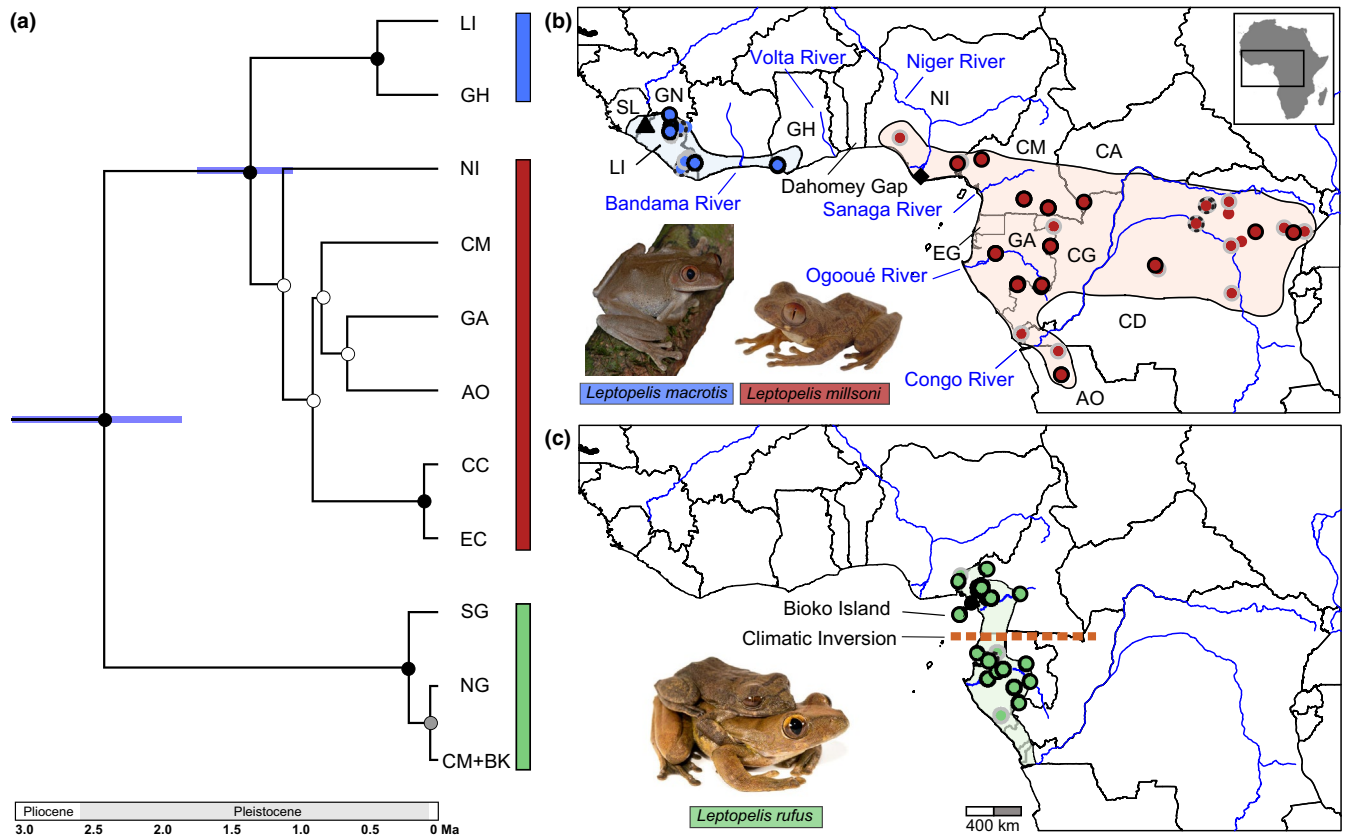
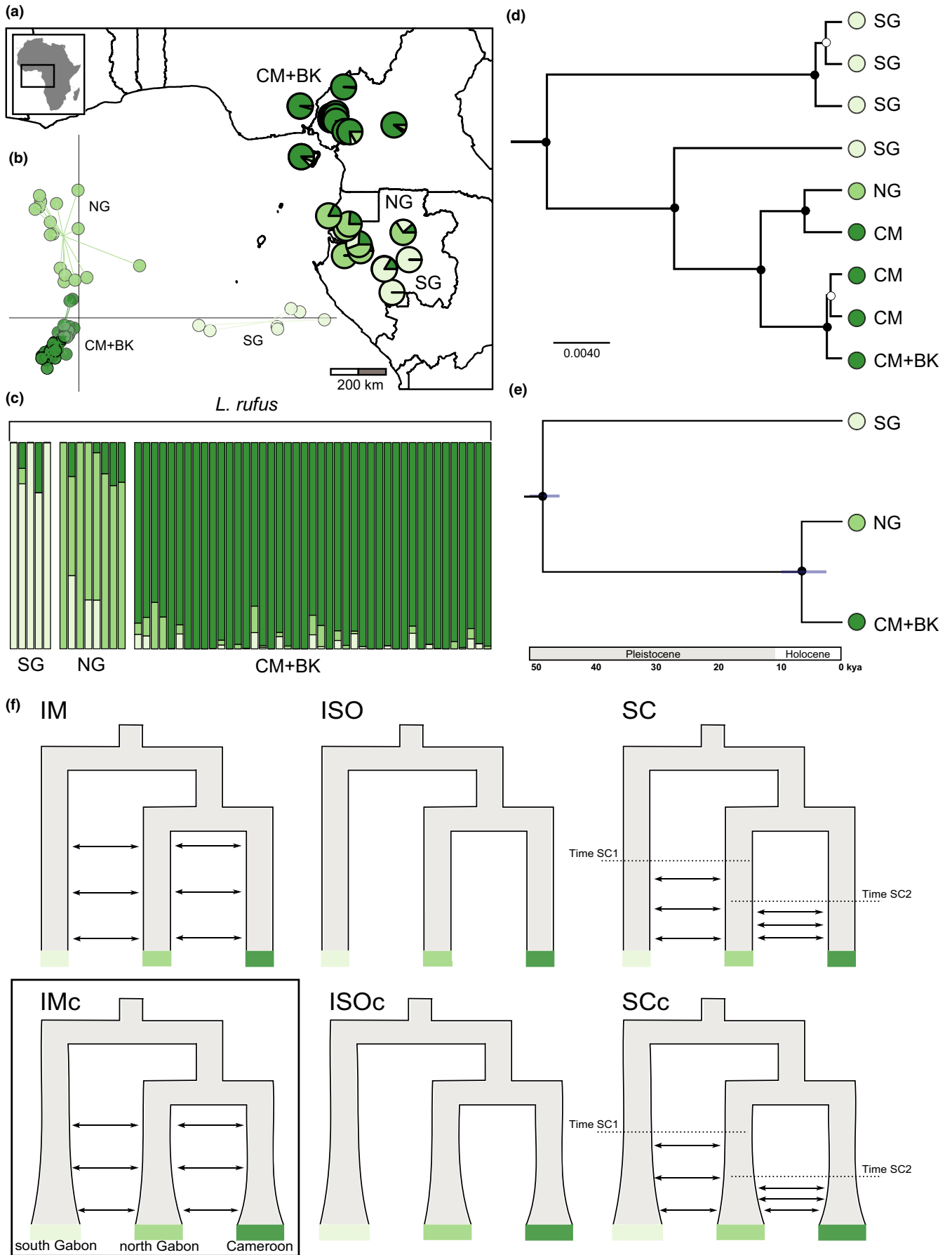


FIGURE 1 Species tree and sampling map of *Leptopelis macrotis*, *L. millsoni*, and *L. rufus*. (a) SNAPP species tree of *L. macrotis*, *L. millsoni*, and *L. rufus* lineages based on ddRADseq data set (1,037 SNPs). Lineage names match those in Figures 2 and 3. Circles on nodes indicate posterior probability (black ≥ 0.95 , grey ≥ 0.90 , and white < 0.90). Sampling and approximate range map (based on Channing & Rödel, 2019) of (b) *L. macrotis* in West Africa (blue) and *L. millsoni* in West and Central Africa (red), and (c) *L. rufus* in Central Africa and Bioko Island (green). Sample borders indicate the type of data sets for each sample: mtDNA, ddRADseq, and morphology (black border), mtDNA and ddRADseq (grey-black dashed border), mtDNA and morphology (grey border), and mtDNA only (no border). Type localities are indicated in black for *L. macrotis* (triangle), *L. millsoni* (diamond), and *L. rufus* (circle). Country abbreviations: AO, Angola; CA, Central African Republic; CD, Democratic Republic of Congo; CM, Cameroon; GA, Gabon; GH, Ghana; GN, Guinea; LI, Liberia; CG, Republic of the Congo; NI, Nigeria; SL, Sierra Leone. Photo credits: Andi Emrich, Brian Freiermuth, Mark-Oliver Rödel

(Fox, 1995). Like most frog species, male *Leptopelis* produce advertisement calls at breeding sites to attract mates (Amiet & Schiøtz, 1974) and differences in advertisement call between recently diverged *Leptopelis* species in the Albertine Rift (~1%–4% mtDNA divergence) suggest that this sexually selected trait is an important premating isolation mechanism in the early stages of speciation

(Portillo & Greenbaum, 2014a, 2014b). In addition, *L. rufus* males produce a unique courtship call and behaviour that has not been described in other *Leptopelis* (Amiet & Schiøtz, 1974). Beyond potential divergence in tympanum size and courtship behaviour, it is unclear if these giant tree frogs differ in other ecological or morphological traits. Thus, this group presents the opportunity to characterize

FIGURE 2 Genetic structure and demographic models for *Leptopelis rufus*. (a) Sampling of *L. rufus* ddRADseq data set with individual assignments to genetic clusters based on sNMF analyses (15,194 SNPs). (b) Discriminant analysis of principal components (DAPC) of ddRADseq data set with colours corresponding to sNMF clusters. (c) Individual assignment probabilities to genetic clusters identified in sNMF from left to right: South Gabon (SG), North Gabon (NG), and Cameroon + Bioko Island (CM+BK). Deme names reflect the geography for the majority of samples within a given cluster and may include samples from other, adjacent countries. (d) 16S mtDNA chronogram (undated) with reduced sampling representing major lineages (complete chronogram in Supporting Information Materials). Colours and labels correspond to sNMF clusters and circles on nodes indicate posterior probability (black ≥ 0.95 and white < 0.95). (e) SNAPP tree of ddRADseq data set (5,328 SNPs). Colours and labels correspond to sNMF clusters, circles on nodes indicate posterior probability (black ≥ 0.95), and divergence estimate with 95% CI bar. (f) Competing demographic models for the history of *L. rufus*. IM, isolation-migration model with gene flow since population divergence and constant effective population sizes; IMc, isolation-migration with gene flow and population size expansion; ISO, population divergence with no gene flow and constant population sizes; ISOc, population divergence with no gene flow and effective population size expansions; SC, divergence with secondary contact after a period of no gene flow and constant population sizes; SCc, divergence with secondary contact and effective population size expansion. 'Time SC' denotes time to secondary contact. The best fit model is surrounded by a black box



multiple axes of diversification in closely related lineages across a range of biogeographic contexts.

In this study, we combine genomic, phenotypic, and ecological approaches to investigate species-level diversification in giant tree frogs across West and Central Africa. Phylogeographic studies in a number of West and Central African taxa support the role of marine incursions, forest refugia, rivers, and ecological gradients in promoting divergence amongst allopatric populations within species (reviewed in Couvreur et al., 2021). Consequently, we also characterize population structure within each of the giant tree frog species and use an integrative approach to identify mechanisms contributing to intraspecific diversification. Specifically, we (1) characterize genomic, ecological, morphological, and advertisement call divergence amongst species to test the hypothesis that biogeographic barriers promoted divergence in allopatry and that phenotypic divergence enables secondary sympatry, and (2) quantify population genetic structure and potential barriers to gene flow within species to differentiate amongst mechanisms proposed for intraspecific divergence in West and Central African forest-dwelling taxa. We synthesize these findings in an integrative framework to investigate how physical barriers, ecological gradients, and reproductive traits contribute to population divergence and speciation.

2 | MATERIALS AND METHODS

2.1 | Sampling details

We obtained 230 tissue samples (17 *Leptopelis macrotis*, 85 *L. millsoni*, 128 *L. rufus*) from 109 localities across West Africa (Ghana, Guinea, Liberia), Central Africa (Angola, Cameroon, Central African Republic, Democratic Republic of Congo, Gabon, Nigeria, Republic of the Congo), and Bioko Island (Equatorial Guinea). This sampling spans the type localities of the focal species (Figure 1). Tissue samples (liver, muscle, or toe clips) were preserved in 95% ethanol, RNAlater, or liquid nitrogen. Voucher specimens are deposited in natural history museum collections (Table S1).

2.2 | Mitochondrial diversity and divergence

We extracted DNA from tissue samples using a DNeasy Blood & Tissue kit (Qiagen Inc.), and polymerase chain reaction (PCR)-amplified and cycle-sequenced a portion of the 16S mitochondrial gene using the primers 16SA and 16SB (see Supporting Information Materials; Palumbi et al., 1991). Sequences were edited using Geneious v.R8.0.04 (Biomatters Ltd.) and are available on GenBank (see Data Availability). To confirm species identifications made in the field, we estimated mtDNA gene trees for *L. rufus* and for our combined sampling of *L. millsoni* and *L. macrotis*. We aligned sequences with MAFFT using the automatic algorithm selection option (auto) (Katoh et al., 2002; Katoh & Standley, 2013) and selected a substitution model with jModelTest 2.1.4 (Darrriba et al., 2012) based on

BIC (HKY +I + G for *L. rufus*, and HKY +I for *L. macrotis*-*L. millsoni*). For phylogenetic inference we used BEAST v1.8 (Drummond et al., 2012) with a constant size coalescent tree prior. For both data sets, two independent analyses were run for 10 million generations each with sampling every 1,000 generations. We assessed convergence and the effective sample size of parameter estimates using Tracer v1.7 (Rambaut et al., 2018) and repeated simulations without sequence data to test the influence of priors on posterior distributions. We discarded a burn-in of 10% prior to generating a maximum clade credibility tree from the remaining 18,000 trees. We pruned each phylogeny to a representative subset of samples for visualization purposes in the main manuscript. Complete phylogenies are in the Supporting Information Materials (Figures S1, S2). We estimated uncorrected pairwise distances between sequences using Geneious vR8.0.04.

2.3 | Restriction-site associated DNA data set collection

We collected double-digest restriction-site associated DNA (ddRADseq) data from 168 samples representing all mtDNA lineages (15 *L. macrotis*, 57 *L. millsoni*, and 96 *L. rufus*) following Peterson et al. (2012) with modifications from Streicher et al. (2014; see Supporting Information Materials). We processed raw Illumina reads (150 bp single end reads) by removing unique molecular identifier overhangs with Trimmomatic v0.38 (Bolger et al., 2014) and conducted additional bioinformatics with STACKS v2.0 (Rochette et al., 2019). We demultiplexed pooled reads and quality filtered raw data using process_radtags, aligned short reads and assembled them into sets of loci (minimum depth coverage of four reads, maximum of two discrepancies) with denovo_map, generated a catalogue of consensus loci, and matched the loci to this catalogue. Due to the diversity within and amongst our focal species, we ran the populations module to generate multiple data sets only retaining loci present in 50% of individuals and one SNP per locus: all *Leptopelis* samples (1,972 SNPs), *L. rufus* only (15,194 SNPs), and *L. macrotis*-*L. millsoni* combined (7,246 SNPs). Raw reads are archived in the NCBI SRA (see Data Availability).

2.4 | Population structure and species tree estimation

As a preliminary assessment of genetic divergence amongst the three species and to check for mismatches between nuDNA and mtDNA assignment that might indicate hybridization, we ran a discriminant analysis of principal components (DAPC; Jombart et al., 2010) with the 1,972 SNP data set using the R package adegenet 1.8 (Jombart, 2008). We also used sparse nonnegative matrix factorization (sNMF; Frichot et al., 2014) implemented in the R package LEA (Frichot & François, 2015) to assess whether individuals in our data set may be admixed between the three focal species. We ran

sNMF with the 1,972 SNP data set, $K = 3$, 100 replicates, and $\alpha = 10,000$.

To compute least-squares estimates of ancestry coefficients and estimate population structure within the *L. rufus* and *L. macrotis-L. millsoni* lineages, we used sNMF with K from 1–8, 100 replicates, and $\alpha = 10$. Because model-based methods for inferring population structure can be biased by minor allele frequencies (Linck & Battey, 2019), we removed singleton SNPs using vcfTools (Danecek et al., 2011). To assess which value of K best fit the number of populations, we compared cross-entropy scores across replicates. We then took a hierarchical clustering approach (e.g. Pritchard et al., 2003) and reran sNMF within each inferred population until the lowest cross-entropy score across runs for a given population was $K = 1$. To assess variation within and amongst groups detected by sNMF and the mtDNA genealogy, and to visualize the clustering of samples with mixed assignment in sNMF, we ran DAPC (Jombart et al., 2010) for *L. rufus* (15,194 SNPs) and *L. macrotis-L. millsoni* (7,246 SNPs) with K fixed to the number of clusters detected in those analyses.

We used SNAPP v1.5 (Bryant et al., 2012) implemented in BEAST v2.6 (Bouckaert et al., 2014) to estimate the phylogenetic relationships amongst populations identified by our clustering and mtDNA analyses. We performed this analysis to investigate species-level and population-level relationships (with a genome-wide SNP data set) and to inform topology for demographic models of divergence scenarios amongst closely related lineages (see below). We conducted these analyses with a subset of samples from all three *Leptopelis* species (1,037 SNPs) as well as analyses with *L. millsoni* and *L. macrotis* combined (3,649 SNPs) and only *L. rufus* (5,328 SNPs). For each population inferred from our hierarchical sNMF and DAPC analyses, we selected two individuals with the least missing data. We converted our vcf file to a nexus file using vcf2phylip v2.0 (Ortiz, 2019) and the R package phrynomics (<https://github.com/bbanbury/phrynomics>). We ran SNAPP for 1,000,000 iterations with mutation rates u and $v = 1.0$, a gamma distribution with $\alpha = 2$ and $\beta = 200$ for the lambda prior, and default values for the snapprior, sampling every 1,000 steps with the first 10% discarded as burn-in. Branch lengths were scaled to estimate relative divergence times using a generation time of one year and a genome-wide mutation rate estimated in humans (1×10^{-8} ; Lynch, 2010); this rate was used because no genome-wide estimates exist for anurans and this approach has been applied in other studies of African frogs (e.g. Charles et al., 2018; Leaché et al., 2019; Portik et al., 2017). We examined convergence using TRACER 1.7 (Rambaut et al., 2018) and generated a maximum clade credibility tree from the post burn-in samples.

2.5 | Divergence in morphology and advertisement call

To assess the extent of morphological divergence amongst species we took 14 measurements that capture head shape and limb variation to the nearest 0.1 mm using Mitutoyo Absolute Digimatic Calipers (see Supporting Information Materials). We measured 96 adult specimens

included in our genetic data set (9 *L. macrotis*, 20 *L. millsoni*, and 67 *L. rufus*). Male and female measurements were analysed separately to account for sexual size dimorphism. Sex was determined by (a) snout–vent length and (b) presence/absence of pectoral glands or ova in preserved specimens. Adults of *Leptopelis* exhibit a wide range of body sizes; thus, to account for allometry across individuals, we corrected morphological measurements (see Supporting Information Materials). We performed a principal component analysis to find the best low-dimensional representation of morphological variation in the data set and compared all 14 measurements separately across species to look for significant differences in individual traits.

We collected measurements of morphological traits proposed to be diagnostic between the species (SVL snout–vent length, TMP tympanum diameter, EYE eye diameter, and DSC disc toepad diameter) from 74 additional specimens included in our genetic data set (5 *L. macrotis*, 32 *L. millsoni*, 37 *L. rufus*) and the type specimens of *L. rufus*, *L. macrotis*, and *L. millsoni*. To quantify divergence in TMP, EYE, DSC and for the composite traits TMP-EYE ratio and DSC-TMP ratio, we fit an ANOVA for each set of traits with measurements grouped by species, and used a Tukey's honest significant differences test to calculate adjusted p -values for group mean comparisons. We conducted the same analyses to quantify divergence in SVL, TMP, EYE and DSC with males and females grouped separately. All statistical analyses were performed in R v3.3.0 and data were visualized using the ggplot2 package (Wickham, 2016).

We obtained recordings of male advertisement calls for *L. macrotis*, *L. millsoni*, and *L. rufus*, and the unique male courtship call of *L. rufus* (Amiet & Goutte, 2017; Rödel et al., 2014). Audiospectrograms and oscillograms were made using Raven Pro 1.4 (Cornell Laboratory of Ornithology), and analysed with a Fast Fourier transformation window of 512 points, a brightness of 70 points, and a contrast of 70 points. The following parameters were measured because they capture the primary axes of variation in *Leptopelis* advertisement calls (Amiet & Goutte, 2017): pulses per call, pulse duration, peak frequency (Hz), frequency range (Hz).

2.6 | Ecological niche modelling, divergence, and suitability through time

We used ecological niche models (ENMs) to estimate the potential geographic distributions of our focal taxa (full details in Supporting Information Materials). Briefly, we used specimen occurrence records confirmed by mtDNA sequence data and thinned with the R package spThin (Aiello-Lammens et al., 2015) such that no records were within 20 km of one another. Sensitivity analyses indicate that species distribution models perform well with 13–25 occurrence points for widespread species and that fewer occurrences are needed to generate reasonable models for species with small ranges (van Proosdij et al., 2016). Given the few confirmed occurrence records for *L. macrotis* and that we aimed to model environmental suitability across the Dahomey Gap for the *L. macrotis-L. millsoni* lineage, we took a more conservative approach by jointly estimating

the ENM for *L. macrotis* and *L. millsoni*. Our sampling localities are not randomly drawn from across the species' ranges; therefore, we applied a similar sampling bias to background points for our ENMs. Following Bell et al. (2017) we selected pseudoabsence background points using a sampling effort surface based on all georeferenced anuran specimen records across sub-Saharan Africa (see <https://github.com/eddiemyers/Leptopelis>).

We used seven uncorrelated bioclimatic variables from WorldClim v1.4 (Hijmans et al., 2005) sampled at 2.5 arcmin resolution. Optimal model parameters for MaxEnt (Phillips et al., 2006) were selected using the R package ENMeval (Muscarella et al., 2014); the best fit parameters were chosen using AIC values. ENMs were constructed with MaxEnt using Biomod2 (Thuiller et al., 2016) in R with 25 evaluation runs, each replicated for 5,000 iterations, reserving 25% of sample localities as a training data set for model evaluation. We created response curves and jackknifed our data to measure variable importance for each ENM. To create binary ENMs at different time periods and to avoid subjective threshold cutoff values for these projections (e.g. Freeman & Moisen, 2008), we used the ROC binary method implemented in Biomod2. We reran the current climate models using this binary projection and hindcast them on climate models of the mid-Holocene (6 kya), the Last Glacial Maximum (21 kya), and the Last Interglacial (120 kya), with the same set of seven uncorrelated variables. To identify core regions of habitat suitability through time for *L. rufus* and *L. macrotis*-*L. millsoni*, we stacked the binary projections for these three time periods plus the current model.

Finally, to investigate whether *L. rufus*, *L. macrotis*, and *L. millsoni* have nonequivalent environmental niches, we used the `enmtools.ecospat.id` function in *ENMTools* (Warren et al., 2019). This method uses kernel density smoothing to estimate species' niche space and corrects for environment availability when measuring overlap between species (Broennimann et al., 2012). A *D* statistic of 1 indicates complete niche overlap and a value of zero indicates no overlap.

2.7 | Isolation by distance, isolation by environment, and demographic model selection

To differentiate amongst mechanisms proposed for intraspecific divergence in West and Central African forest-dwelling taxa, we tested for isolation-by-distance and isolation-by-environment within *L. rufus*, *L. macrotis*, and *L. millsoni* with generalized dissimilarity modelling (GDM; Ferrier et al., 2007), a matrix regression technique that models variation between distance matrices and fits nonlinear relationships between these matrices (Ferrier et al., 2007). We chose this method because there is unlikely to be a linear correlation in this study system between increasing genetic distance and either ecological or geographical distance between sampling localities. To test for isolation-by-environment within each species, we used the seven Bioclim variables from the ENMs (see above) and extracted environmental variation from each locality in the respective SNP data sets. Genetic distance matrices were calculated using Nei's *D* distances (Nei, 1972) in *adegenet* (Jombart, 2008). We fit

generalized dissimilarity models in the GDM R package (Manion et al., 2016) using genetic distance matrices as the response variable and geographic and climate distances as the explanatory variables. We then used matrix permutation to perform model and variable significance testing and to estimate variable importance (percent deviation explained by each variable), using the GDM R package.

Methods that explicitly quantify demographic changes in population size and gene flow can help to differentiate amongst potential mechanisms contributing to lineage diversification (Portik et al., 2017). We conducted demographic model selection analyses within *L. rufus* but did not have sufficient population-level sampling to conduct parallel analyses within *L. macrotis* or *L. millsoni*. To investigate diversification within *L. rufus*, we tested six, three-population demographic models using `fastsimcoal2` (`fsc2`; v2.6.0.2, Excoffier et al., 2013), which uses coalescent simulations to approximate an expected site frequency spectrum (SFS) and a composite likelihood approach for parameter optimizations. The six demographic models were constructed to test if lineage divergence within *L. rufus* was consistent with strict allopatric divergence (ISO model, e.g. across major rivers like the Ogooué or Sanaga) versus repeated bouts of isolation-migration or divergence with secondary contact (IM and SC models, e.g. ecological gradients or climatic refugia), with either constant population size (ISO, IM, SC models) or population size change (IMc, ISOc, SCc models, e.g. expansion/contraction in response to climate). These models differed in the parameterization of gene flow (between geographically adjacent lineages), timing of gene flow, and population size change (Figure 2), and whilst they are simplifications of the true underlying demographic history, they allow us to distinguish between these broad scenarios of diversification (e.g. Myers et al., 2020; Portik et al., 2017). To construct the SFS, we used `easySFS` (<https://github.com/isaacovercast/easySFS>) and downsampled the full data set to a smaller number of samples per population to reduce missing data and maximize the number of segregating sites. Furthermore, because of the assumptions of `fsc2`, we projected the SFS as haploid data. For all models we fixed the topology of the *L. rufus* lineages based on the SNAPP results. We ran 100 replicate `fsc2` analyses for each model, with 100,000 simulations to estimate the composite likelihood and 40 ECM cycles for parameter optimization per run. For each model we calculated the AIC from the approximated likelihood and ranked models based on Δ AIC and AIC weights. All input files are available at github.com/eddiemyers/Leptopelis. For the best-fit model we performed 20 parametric bootstraps to produce parameter estimates with a generation time of one year and a genome-wide mutation rate of 1×10^{-8} .

3 | RESULTS

3.1 | Mitochondrial diversity and divergence

The mtDNA phylogeography of *L. rufus* indicated deep divergence across its distribution (up to 5.7% uncorrected pairwise distance; Figures 1, 2, Supporting Information 1). Samples of *L. rufus* from

Bioko Island formed a clade with samples from adjacent Cameroon and Nigeria, and exhibited very low sequence divergence from these mainland samples (0.2%–0.4% uncorrected pairwise distance; Figure S1). The 16S mtDNA genealogy indicated extensive structure across the distribution of *L. macrotis*–*L. millsoni* (up to 4.3% uncorrected pairwise distance), but relationships amongst many lineages were poorly supported (Figures 1, 3, Supporting Information 2). Given the low support for many nodes in the *L. macrotis*–*L. millsoni* phylogeny, as well as differences in topology between mtDNA and nuDNA phylogenies (see below), we did not estimate divergence times for the mtDNA data sets.

3.2 | SNP data set

We generated approximately 180 million sequence reads after filtering for quality, intact restriction sites, and matches to sample barcodes (average 1.7 million reads per sample). We dropped 24 samples with <500,000 reads after initial quality filtering. The resulting data set still included representatives from all mtDNA lineages. The STACKS pipeline generated a catalogue of 687,815 unique loci for 144 samples. We retained loci with <50% missing data, trimmed individuals with >90% missing data with Matrix Condenser v.1.0. (de Medeiros, 2019), and selected one SNP per locus, resulting in three final data sets: all *Leptopelis* species (1,972 SNPs, $N = 108$), *L. rufus* (15,194 SNPs, $N = 56$), and *L. macrotis*–*L. millsoni* (7,246 SNPs; $N = 10$ *L. macrotis*, $N = 42$ *L. millsoni*).

3.3 | Population structure and species tree estimation

DAPC clustering with the 1,972 SNP data set did not indicate mismatches between nuDNA and mtDNA assignments amongst the three species despite *L. rufus* and *L. millsoni* co-occurring in direct sympatry at breeding sites in Cameroon and in Gabon (Figure S3). The interspecific sNMF analysis assigned nearly all individuals to one of the three species with high ancestry coefficients (Figure S3D). The one exception was a specimen of *L. millsoni* (NMP:P6V:76050) with proportions of ancestry from both *L. millsoni* and *L. rufus*; however, this specimen was collected outside the current distribution of *L. rufus* and had ~79% missing data in the all species SNP data set. Thus, we interpret this mixed assignment as low posterior probability rather than admixture.

Hierarchical population structure analyses for *L. rufus* using sNMF indicated $K = 3$ as the best fit and corresponded to the mtDNA gene tree and DAPC groups (Figure 2, Supporting Information 4). For *L. millsoni* and *L. macrotis*, we found that $K = 7$ was the best fit and these groupings corresponded to the mtDNA lineages (Figures 3, S5). DAPC clustering with seven genetic groups aligned with sNMF results except for one difference: DAPC lumped Central and Eastern Congo samples whereas the Angola samples formed a distinct genetic group (Figure 3). DAPC analyses with eight groups found the

same genetic groups as sNMF with the addition of Angola. Thus, although samples from Angola had mixed assignment in sNMF, we treated them as a separate group in our species tree analysis based on their distinctiveness in mtDNA and the DAPC analysis (Figure 3, see below).

The species tree estimating interspecific relationships was strongly supported with posterior probabilities of 1.0 (Figure 1). The divergence time estimated between *L. rufus* and *L. macrotis*–*L. millsoni* was in the early Pleistocene (2.45 million years ago [Ma], CI: 1.74–3.1 Ma) followed by divergence between *L. macrotis* and *L. millsoni* (1.37 Ma, CI: 1.1–1.7 Ma; Figure 1). In contrast to the mtDNA analyses, both nuDNA phylogenies (e.g. with all taxa and with only *L. macrotis*–*L. millsoni*) supported reciprocal monophyly of *L. millsoni* and *L. macrotis* (Figure 3). In both analyses, the oldest lineage within *L. millsoni* was the Nigerian population, but the placement of this lineage was not well supported (PP = 0.64–0.66). Our divergence time estimates indicate that population level divergence within all three species occurred throughout the Pleistocene and into the Holocene (Figures 2, 3).

3.4 | Divergence in morphology and advertisement calls

For males and females of all three species, much of the variance in morphology was captured in the first two principal components (53% and 50%, respectively; Figure 4a, Tables S2, S3, S4 and Supporting Information Materials) with broad overlap in PC space amongst males and moderate separation amongst females, although sample sizes were smaller for females than males. We found limb measurements exhibited minor differences between species in both sexes whereas head measurements did not differ (Table S5). With respect to the proposed diagnostic morphological measurements, we found that tympanum diameter (TMP) and the toepad disc-tympanum diameter (DSC-TMP) and tympanum-eye diameter (TMP-EYE) ratios differed significantly in *L. rufus* compared to *L. macrotis* and *L. millsoni* across both males and females (Figures 4b, S6). Overall, TMP was smaller in *L. rufus* relative to the other species ($p < .05$) and DSC-TMP was consistently >3:4 in *L. rufus* and <3:4 in the other species ($p < .05$; Figure 4b). Likewise, TMP-EYE was consistently <1:2 in *L. rufus* and >1:2 in the other species ($p < .05$; Figure 4b). TMP-EYE also differed significantly between *L. macrotis* and *L. millsoni* females but not males ($p < .05$; Figure S6). Finally, we found significant differences in male SVL amongst all three species and that female *L. macrotis* were significantly larger than *L. millsoni* females but not *L. rufus* females ($p < .05$; Figure S6).

The advertisement calls of *L. macrotis*, *L. millsoni* and *L. rufus* differed with respect to average peak frequency and frequency range, as well as the number and duration of pulses (Table 1, Figure S7). Male *L. macrotis* produced calls at lower peak frequencies (~1,700 Hz), *L. millsoni* at intermediate peak frequencies (~2,100 Hz), and *L. rufus* at higher frequencies (~2,800 Hz or higher). The peak frequency of the unique *L. rufus* courtship call was also high (>2,200 Hz) and the

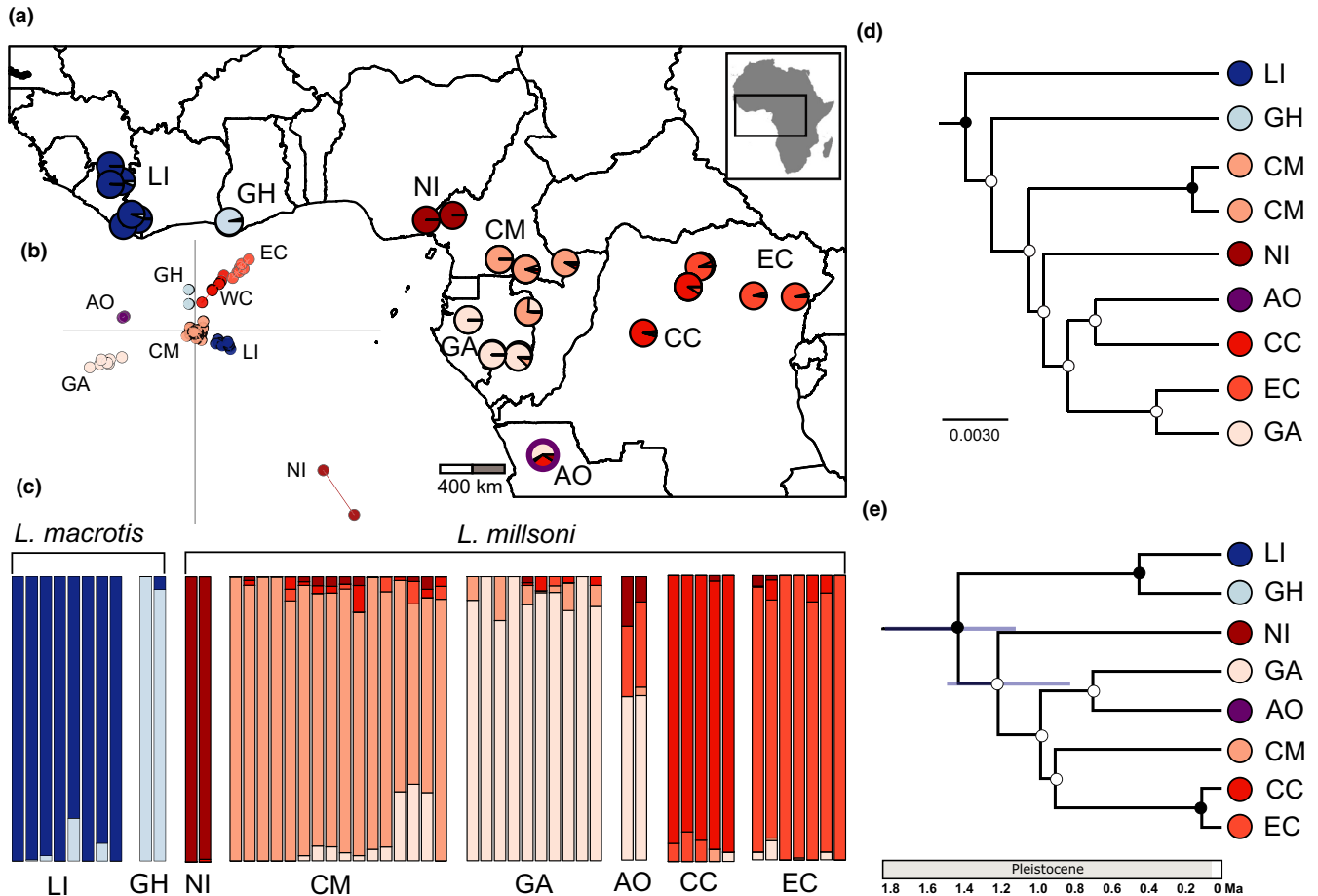


FIGURE 3 Genetic structure in *Leptopelis macrotis* and *L. millsoni*. (a) Sampling of *L. macrotis* and *L. millsoni* ddRAD data sets with individual assignments to genetic clusters based on sNMF analyses (7,246 SNPs). (b) Discriminant analysis of principal components (DAPC) of ddRADseq data set with colours corresponding to sNMF clusters. Note that samples from Angola (AO) had intermediate assignment probability in sNMF and were treated as a separate group in the DAPC. These samples are purple in the DAPC plot. (c) Individual assignment probabilities to genetic clusters identified in sNMF from left to right: *L. macrotis* (Liberia [LI], Ghana [GH]), *L. millsoni* (Nigeria [NI], Cameroon [CM], Gabon [GA], Angola [AO], Central Congo [CC], and East Congo [EC]). Deme names reflect the geography for the majority of samples within a given cluster and may include samples from other, adjacent countries. (d) 16S mtDNA chronogram (undated) with reduced sampling representing major lineages (complete chronogram in Supporting Information Materials). Colours and labels correspond to sNMF clusters and circles on nodes indicate posterior probability (black ≥ 0.95 and white < 0.95). (e) SNAPP tree of ddRADseq data set (3,649 SNPs). Colours and labels correspond to sNMF clusters, circles on nodes indicate posterior probability (black ≥ 0.95 and white < 0.90), and divergence estimates with 95% CI bars

duration of each note was >1.5 s (Table 1). Advertisement calls of *L. macrotis* included notes with 1–2 pulses whereas the calls of *L. millsoni* and *L. rufus* had single pulsed notes.

3.5 | Ecological niche and suitability through time

After thinning locality records, we retained a total of 36 and 21 unique localities for *L. macrotis*-*L. millsoni* and *L. rufus*, respectively. The best-fit combinations of parameters differed between the two models, with a combination of feature classes of 'LQHPT' and a regularization multiplier of 3.5 for *L. macrotis*-*L. millsoni* and a feature class 'H' and regularization multiplier of 2 being best-fit for *L. rufus*. MaxEnt models performed well: *L. macrotis*-*L. millsoni* AUC = 0.92, *L. rufus* AUC = 0.98. Annual precipitation had the greatest percent

contribution, approximately 0.75, to ENMs for both lineages (Table S6). The current ENM for *L. macrotis*-*L. millsoni* predicted the known geographic distribution of this group; however, the models did not predict high suitability in much of western Central Africa (Figure 5a). The ENM for *L. rufus* predicted a somewhat wider geographic distribution than is known for this taxon with potentially suitable environments along the mouth of the Niger River and in West Africa, where *L. macrotis* occurs (Figure 5b). The ENMs predicted suitable habitat for both *L. rufus* and the *L. macrotis*-*L. millsoni* lineage on Bioko Island, yet only *L. rufus* is confirmed to occur there.

In our stacked suitability maps overlaying current suitability models with the mid-Holocene (6 kya), Last Glacial Maximum (21 kya), and Last Interglacial (120 kya) models, we found two core regions of stability in West Africa corresponding to the distribution of *L. macrotis*. Likewise, we found extensive suitability through time across the

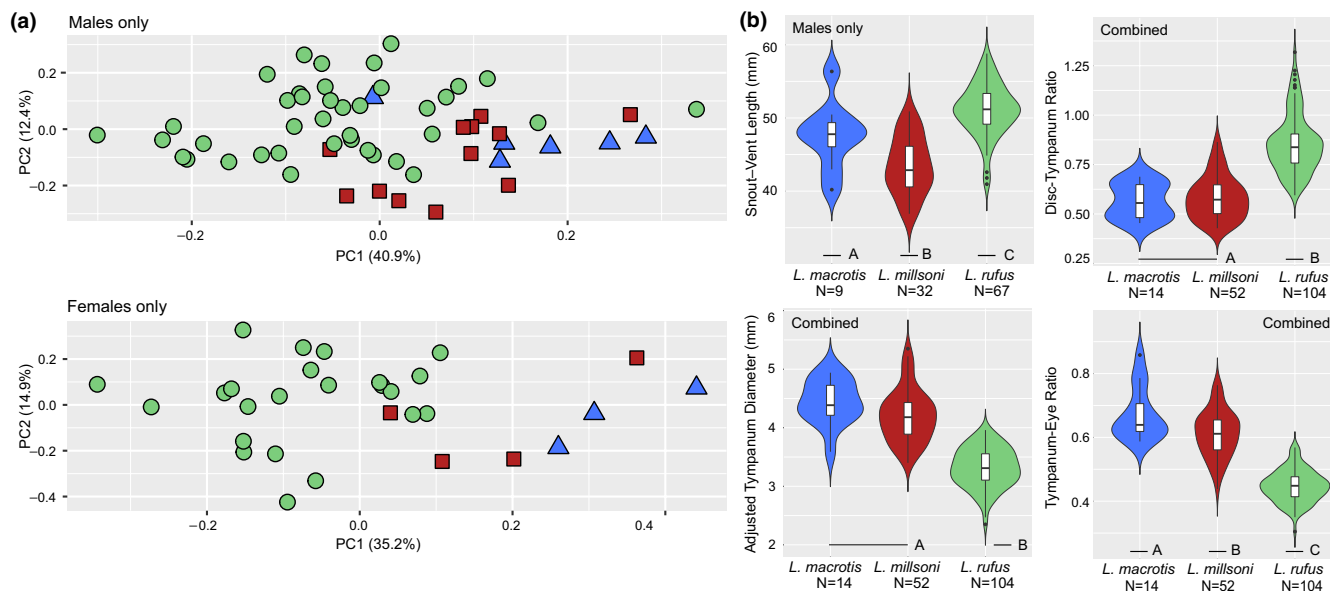


FIGURE 4 Morphological variation and divergence amongst *Leptopelis macrotis*, *L. millsoni* and *L. rufus*. (a) Principal component analysis (PCA) of 14 morphological measurements for males and females of *L. macrotis* (blue triangle), *L. millsoni* (red square), and *L. rufus* (green circle). (b) Violin plots of male snout-vent length, and combined male and female size-adjusted tympanum diameter, disc-tympanum ratio, and tympanum-eye ratio. Boxes within violin plots signify first quartile, median, and third quartile. Comparisons significant at an adjusted $p < .05$ with a Tukey's honest significant difference test are indicated by letters

present distribution of *L. millsoni* and centred in the Lower Guinean Forests and Congo basin (Figure 5c). By contrast, the region presently known as the Dahomey Gap seems to have remained unsuitable for *L. millsoni* and *L. macrotis* throughout the Quaternary (Figure 5c). Within the current geographic distribution of *L. rufus*, our models identified core regions of suitability in coastal Nigeria/Cameroon and southern Gabon that are separated by lower suitability within Equatorial Guinea and northern Gabon (Figure 5d). Projections for individual time periods are in the Supporting Information Materials (Figures S8, S9).

Niche equivalency tests demonstrated that all three species occupy distinct environmental niches with moderate overlap between *L. millsoni* and *L. macrotis* (D statistic 0.22, I statistic 0.33, $p < .02$), and low overlap between *L. rufus* and *L. macrotis* (D statistic 0.04, I statistic 0.18, $p < .01$) and *L. rufus* and *L. millsoni* (D statistic 0.02, I statistic 0.11, $p < .01$).

3.6 | Isolation by distance, isolation by environment, and demographic model selection

Generalized dissimilarity models for each species demonstrated that geographic distance between sampled localities was a significant determinant of population genetic structure. In *L. millsoni* the best fit model included both geographic distance and annual precipitation with variable importance 64.4% and 16.7%, respectively ($p < .01$). For *L. macrotis*, a model including geographic distance and mean diurnal temperature range predicted genetic distances (variable importance 1.5% and 4.6%; $p < .01$). Finally, within *L. rufus* the only

explanatory variable that predicted population genetic distances was geographic distance (variable importance 48.6%; $p < .05$).

Downsampling the *L. rufus* populations for demographic model selection resulted in six haploid samples from southern Gabon (SG), 12 from northern Gabon (NG), and 65 from Cameroon (CM+BK). Our uneven sampling amongst the three populations could bias our estimates of genetic diversity and gene flow. However, our primary motivation for conducting these analyses was to select the best-fit model of lineage divergence and secondarily, to compare estimates of divergence time with those obtained from SNAPP. We found strong support for a model of isolation-migration with population size change (IMc; AIC-weight 0.99; Figure 2, Table S7). This model of continuous gene flow, or repeated bouts of isolation and contact between lineages, with growth in effective population size is consistent with allopatric or parapatric divergence in response to a dynamic climatic history. Under this best-fit model, the estimated mean divergence time for the initial split in *L. rufus* is 898 kya (95% CI: 711–1,084 kya) and the divergence time between the Cameroon and northern Gabon lineages is 570 kya (461–680 kya) (Tables S7, S8). These dates are much older than those inferred by SNAPP; however, gene flow between lineages is a violation of the coalescent model in SNAPP (Bryant et al., 2012) and thus we place more confidence in divergence times estimated from fsc.

4 | DISCUSSION

Our analyses indicate that *L. macrotis*, *L. millsoni*, and *L. rufus* diverged in the late Pliocene to early Pleistocene with no evidence

TABLE 1 Summary of parameters for *L. macrotis*, *L. millsoni*, and *L. rufus* male advertisement calls, and *L. rufus* male courtship call

Species	Location	N	APPC	ADF (Hz)	FR (Hz)	APD (s)	Recording source
<i>L. macrotis</i> advertisement 1	Ivory Coast	11	1.8 (1-2)	1,696 (1,421-1,744)	1,400-2,400	0.09 (0.08-0.12)	Rödel et al., 2014
<i>L. macrotis</i> advertisement 2	Ivory Coast	1	2	1,723	1,400-2,400	0.11 (0.10-0.12)	Rödel et al., 2014
<i>L. macrotis</i> advertisement 3	Ivory Coast	8	1.9 (1-2)	1,724 (1,695-1,782)	1,400-2,500	0.12 (0.10-0.17)	Rödel et al., 2014
<i>L. millsoni</i> advertisement 1	Cameroon, Avebe, Soo River, swamp forest	5	1	2,257 (2,067-2,325)	1,300-4,200	0.12 (0.10-0.14)	Amiet & Goutte, 2017
<i>L. millsoni</i> advertisement 2	Cameroon, Messam, Awout River, swamp forest	7	1	2,116 (2,067-2,153)	400-14,500+	0.12 (0.11-0.13)	Amiet & Goutte, 2017
<i>L. rufus</i> advertisement 1	Cameroon, Ototomo, small stream	6	1	2,857 (2,756-3,359)	1,100-6,500	0.24 (0.22-0.26)	Amiet & Goutte, 2017
<i>L. rufus</i> advertisement 2	Cameroon, Kala Afomo, forest clearing	7	1	3,248 (2,842-3,962)	600-6,000	0.23 (0.23-0.24)	Amiet & Goutte, 2017
<i>L. rufus</i> courtship	Cameroon, Ebone, small stream	3	1	3,101 (2,239-3,531)	1,750-5,100	1.71 (1.53-1.83)	Amiet & Goutte, 2017

Abbreviations: ADF, average dominant frequency; APD, average pulse duration; APPC, average pulses per call; FR, frequency range; N, notes analysed.

of current gene flow between species. The distributions of *L. macrotis* and *L. millsoni* appear to be entirely allopatric on either side of the Dahomey Gap in West Africa. By contrast, our results indicate the distributions of *L. rufus* and *L. millsoni* are broadly parapatric in Central Africa and we confirm that the species co-occur in direct sympatry at breeding sites in Cameroon and Gabon. All three species occupy distinct environmental niches with moderate overlap between *L. millsoni* and *L. macrotis*. Despite long periods of isolation and evidence of ecological divergence, phenotypic differentiation amongst the species is modest with the exception of divergence in body size, tympanum diameter, and advertisement call. At the intraspecific level, we find extensive phylogeographic structure that largely coincides with centres of current and historic climatic suitability in *L. macrotis* and *L. rufus*. Model-based inferences for *L. rufus* were consistent with divergence between regions of consistently suitable climate. Our sampling did not permit model-based inferences for *L. macrotis* or *L. millsoni*, but our other analyses indicate that phylogeographic structure in these taxa may result from a combination of isolation-by-distance, riverine barriers, climatic refugia, and precipitation gradients. Below we discuss genomic, environmental, and phenotypic divergence with respect to inter- and intraspecific diversification in the giant tree frogs.

4.1 | The geography of speciation in the giant *Leptopelis* tree frogs

The earliest divergence amongst our focal species occurred in the late Pliocene to early Pleistocene (~2.5 Ma) with subsequent divergence between *L. macrotis* and *L. millsoni* in the mid Pleistocene (~1.4 Ma). This time period coincides with the onset of glacial-interglacial cycles that strongly impacted the distribution of vegetation types across Africa (Trauth et al., 2009) including cycles of isolation and connectivity between West and Central African forests (Bonnefille, 2010; Dupont et al., 2000). In particular, pollen records indicate that the Pliocene-Pleistocene transition (~2.7 Ma) was characterized by very low tree cover (Bonnefille, 2010) in contrast to the expansive tropical forests of the mid-Pliocene (~5-3 Ma; Morley, 2000). Phases of connectivity are hypothesized to have enabled faunistic exchanges between West and Central Africa followed by additional periods of geographic isolation (reviewed in Couvreur et al., 2021). Based on the topology of inter- and intraspecific divergences in the giant tree frogs, we infer that large-scale forest fragmentation during this time period resulted in disjunct distributions of a previously more widespread lineage of forest-dwelling giant tree frog into refugia in West (*L. macrotis*-*L. millsoni*) and Central (*L. rufus*) Africa. After this initial period of divergence, we propose that populations of the *L. macrotis*-*L. millsoni* lineage became isolated on either side of the Dahomey Gap (1.1-1.7 Ma). Although palynological data imply rainforest habitat was continuous through this region during the wetter periods of the Holocene (Dupont et al., 2000), our ENMs indicate that environmental conditions within the Dahomey Gap were less suitable for our focal taxa in the four time periods we projected, including the

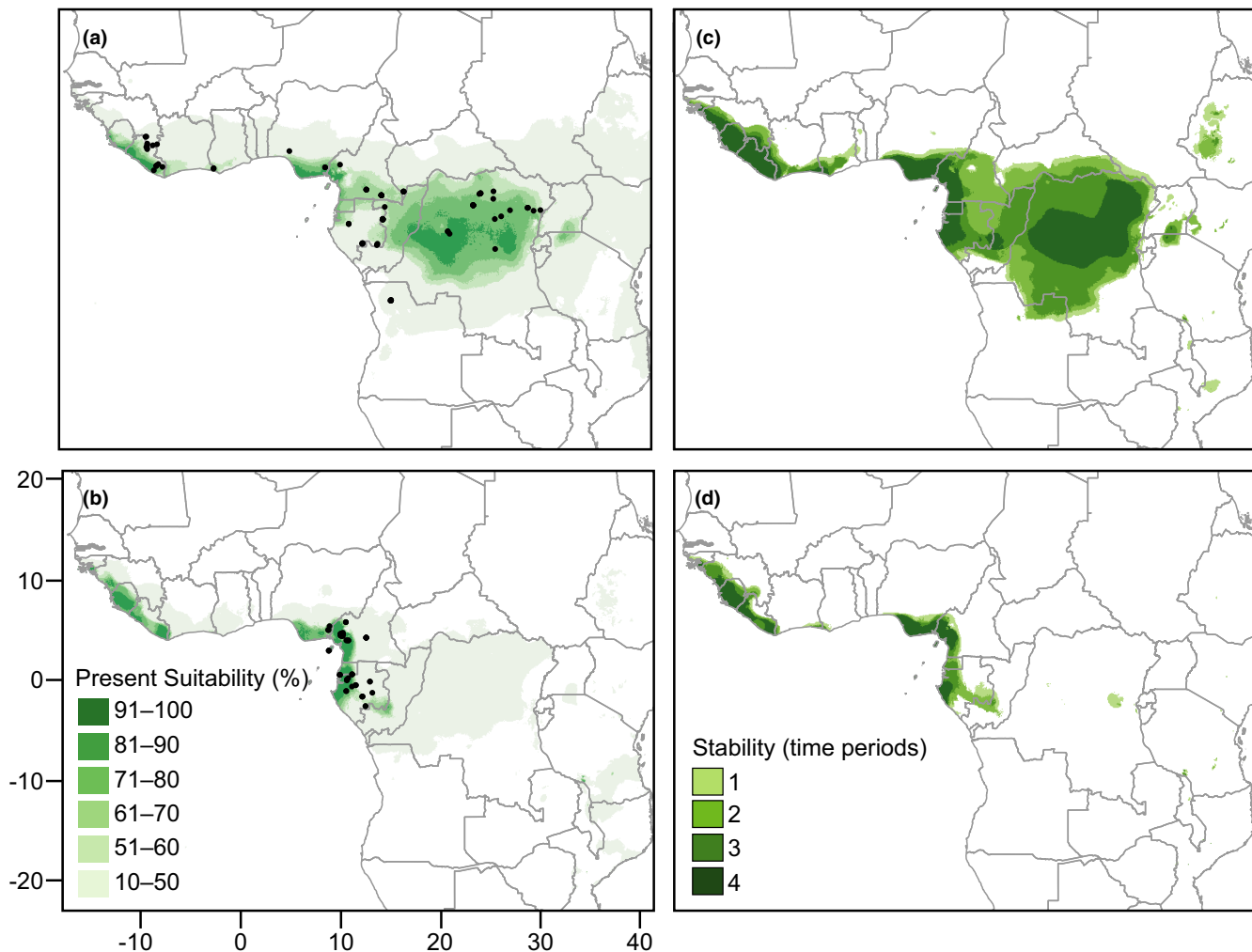


FIGURE 5 Ecological niche models for *Leptopelis macrotis*-*L. millsoni* and *L. rufus*. Distribution of current suitable climates for *L. macrotis*-*L. millsoni* (a) and *L. rufus* (b), black dots indicate thinned sampling localities used to generate the models. Estimated suitable climate stability summed across four time periods (1) present, (2) mid-Holocene (6 kya), (3) Last Glacial Maximum (21 kya), and (4) the Last Interglacial (120 kya) for *L. macrotis*-*L. millsoni* (c) and *L. rufus* (d). Note the study area for the modelling analysis included all of sub-Saharan Africa (including continental islands) but maps were cropped for visualization

mid-Holocene. These results are consistent with our molecular data and we infer that this region has acted as a biogeographic barrier for the species since the mid-Pleistocene. Phylogeographic structure within *L. millsoni* suggests this lineage subsequently expanded east and south across Central African forests resulting in a broadly parapatric distribution with *L. rufus*. Furthermore, although distribution maps of *L. millsoni* illustrate this species range as occurring throughout the distribution of *L. rufus* (e.g. Channing & Rödel, 2019), our genetically confirmed occurrence records of *L. millsoni* suggest that the species does not occur within the core of the *L. rufus* range in western Gabon and Cameroon.

This evolutionary history and geographic distribution would imply that *L. rufus* and *L. millsoni* diverged in allopatry and that divergence in ecological and/or reproductive traits enabled these closely related species to coexist in secondary sympatry. Several studies amongst closely related species of birds found similar patterns, with phenotypic and/or ecological divergence amongst close relatives

that occur in secondary sympatry (e.g. Friis & Milá, 2020; Krishnan & Tamma, 2016; Pigot & Tobias, 2015). These patterns support the hypothesis that biotic interactions play an important role in determining species distributions through space and time, and ultimately in the accumulation of species richness. Future studies characterizing physiological breadth, competitive interactions, and premating isolation barriers amongst our focal species would clarify which of these biotic mechanisms contribute to their present distributions. In addition, further population genomic sampling across the distribution of *L. millsoni*, coupled with methods that explicitly test for demographic expansion and gene flow would clarify the temporal and geographic extent of secondary sympatry with *L. rufus*.

Several phylogenetic studies of rainforest taxa that span West and Central Africa also report late Pliocene/early Pleistocene divergence times, suggesting this period played an important role in structuring current species diversity across taxonomic groups. For instance, patterns of inter- and intraspecific genetic divergence in

Scotonycterini fruit bats mirror those of the giant tree frogs with two phases of allopatric speciation (~2.7 and ~1.6 Ma) attributed to forest refugia in West and Central Africa (Hassanin et al., 2015). Similar patterns are also documented in pangolins (Gaubert et al., 2018), bristlebill birds (Huntley & Voelker, 2016), wood mice (Nicolas et al., 2020), swamp rats (Bohoussou et al., 2015), and foam-nest tree frogs (Leaché et al., 2019), in which inter- and intraspecific diversification spanning West and Central Africa dates to the Pliocene and Pleistocene. This emerging pattern across taxonomic groups indicates these recurrent cycles of isolation and exchange across West and Central Africa likely contributed to high regional species diversity. Likewise, a number of closely related species-pairs exhibit distributions similar to *L. rufus* and *L. millsoni* in Central Africa including reed frogs (Bell et al., 2017), bristlebills (Huntley & Voelker, 2016), and fruit bats (Hassanin et al., 2015). In these taxa, western-Central and eastern-Central lineages meet at the boundaries of the Lower Guinean and Congolian forests, coinciding with a longitudinal precipitation gradient from high rainfall and lower seasonality along the Atlantic coast, and more variable precipitation and seasonality moving inland (Heuertz et al., 2014; Olson et al., 2001). Annual precipitation had the greatest percent contribution to ENMs for *L. millsoni* and *L. rufus*, and we found that only western-Central forests provided suitable climates for *L. rufus* whereas a wider climatic range and geographic area were suitable for *L. millsoni*. ENMs for reed frogs (Bell et al., 2017) revealed parallel patterns of environmental niche breadth and suitability for western-Central versus eastern-Central African sister taxa, suggesting that divergence in environmental niche amongst close relatives further contributes to regional species diversity. These shared patterns of divergence amongst diverse taxa in the West and Central African forests provide a compelling comparative framework for future studies investigating abiotic and biotic mechanisms of lineage divergence and species accumulation.

4.2 | Divergence in morphological, acoustic, and ecological traits amongst giant tree frogs

Although *L. millsoni* and *L. rufus* are closely related and phenotypically similar, we did not find any evidence of hybridization despite collecting multiple individuals of each species side-by-side at two breeding sites (Cross River, Nigeria; Baposo village, Ngounié, Gabon). Hybridization and the persistence of genetic compatibility between even distantly related amphibians is common (Wilson et al., 1974); consequently, we propose that the few distinguishable differences in ecology, morphology, and courtship between *L. millsoni* and *L. rufus* may serve as prezygotic barriers to hybridization in sympatry. For instance, *L. millsoni* typically form large breeding choruses along slow-moving rivers and swamps where males produce louder calls at lower frequencies, whereas in *L. rufus* solitary males produce soft, higher frequency calls above fast-flowing streams in the forest (Amiet & Schiøtz, 1974). Furthermore, the distinctive courtship call and behaviour of *L. rufus* has not been documented in other *Leptopelis* and appears to be unique to this species (Amiet & Schiøtz,

1974). Our sampling at sympatric sites is fairly limited and given their broadly parapatric distributions, we suspect that *L. millsoni* and *L. rufus* co-occur at several additional sites along the boundary of the Lower Guinean and Congolian forests. Future studies characterizing habitat preferences, seasonal activity, courtship behaviour, and female preferences in allopatry versus in sympatry would improve our understanding of prezygotic and postzygotic reproductive barriers between these closely related species (e.g. Boul et al., 2006; Uy & Borgia, 2000; Xu & Shaw, 2020).

In most anurans, the frequency of male advertisement calls is inversely correlated with body size such that larger frogs produce lower frequency calls (Gingras et al., 2013; Hoskin et al., 2009). The pattern in the giant tree frogs, however, appears to deviate from this trend. *Leptopelis rufus* males, which are significantly larger, produce higher frequency calls than the smaller-bodied *L. macrotis* and *L. millsoni*. Likewise, tympanum size is often positively correlated with body size in anurans (Fox, 1995), but the larger-bodied *L. rufus* have smaller tympana than *L. macrotis* and *L. millsoni*. This pattern is particularly pronounced in the very large females of *L. rufus*. Tympanum size in anurans has functional consequences for auditory sensitivity such that most measures of sensitivity increase with tympanum area (Fox, 1995). For instance, in bullfrogs, males have larger tympana than females and are sensitive to low-frequency peaks in calls (200–300 Hz) that serve as male-male communication channels (Hetherington, 1994). We propose that paired divergence in tympanum diameter and the frequency of male advertisement calls may play a role in prezygotic isolation between *L. millsoni* and *L. rufus*. More broadly, the giant tree frogs present an exciting study system for investigating the links between the morphology of auditory structures and corresponding sensitivity, divergence in advertisement call, and variation in signalling environment amongst closely related species (e.g. Lattenkamp et al., 2021).

4.3 | Core regions of suitable climate align with intraspecific diversification in *L. rufus*

The distribution of *L. rufus* spans several prominent biogeographic barriers including the Sanaga River in Cameroon, the Ogooué River in Gabon, the climatic hinge between southern Cameroon and northern Gabon, and the marine incursion that presently separates Bioko Island from the rest of the continent. Surprisingly, none of these features appears to be strong barriers to gene flow for *L. rufus*. Our ENMs for *L. rufus* indicated that the species is tied to climates with high annual precipitation, suggesting that north-to-south or east-to-west gradients in precipitation could lead to reduced dispersal across the species range as proposed in other plant and animal taxa (Helmstetter, Amoussou, et al., 2020; Helmstetter et al., 2020; Leaché et al., 2019). Generalized dissimilarity models, however, did not find support for isolation-by-environment and instead indicated an overall pattern of isolation-by-distance across the species distribution. Furthermore, demographic model selection for *L. rufus* determined that isolation-migration with population size change was

the best fit to the data, and this demographic history is more consistent with divergence in response to a dynamic climate history than divergence along an ecological gradient. Our ENMs indicate regions of consistently suitable climate whose locations roughly correspond with the genetic lineages of *L. rufus*. These proposed core regions of stability overlap with projected environmental stability for other forest associated amphibians in this region including several species of reed frog (Bell et al., 2017), the Gaboon forest frog (Portik et al., 2017), and foam-nesting tree frogs (Leaché et al., 2019). Our divergence estimates amongst the three lineages of *L. rufus* range from the mid to late Pleistocene, and roughly coincide with estimates of intraspecific divergence for other anurans across this region that were obtained using similar approaches (i.e. ddRADseq and the same mutation rate; Charles et al., 2018; Portik et al., 2017).

Our sampling for *L. rufus* does not include localities from continental Equatorial Guinea or southern Cameroon. This limits our understanding of where the Cameroon and Northern Gabon lineages meet and may also impact our inferences of environmental niche and isolation-by-distance. Both our mtDNA and nuDNA data sets indicated that these lineages are closely related with the most geographically proximate individuals revealing mixed assignments in our clustering analysis and closely related mtDNA haplotypes. Our ENMs of present suitability suggest that the current environment across the climatic hinge is suitable for *L. rufus*, but our estimates of historical stability suggest lower suitability across this region under past climates. This pattern of lower stability is also evident in ENMs of other forest associated species including the rainforest reed frog (Bell et al., 2017) and foam-nesting tree frogs (Leaché et al., 2019). Consequently, although genetic structure between Cameroon and Gabon populations of *L. rufus* may partly reflect the limitations of our sampling, both our demographic modelling analyses and ENMs support a period of allopatric divergence with more recent demographic expansion and secondary contact that are consistent with divergence in response to a dynamic climate history.

Both our mtDNA and nuDNA analyses indicated that *L. rufus* on Bioko Island clusters with populations from adjacent Cameroon although the Bioko individuals form a monophyletic group in the mtDNA gene tree. This pattern suggests that *L. rufus* on the island have only recently become isolated from the rest of their continental distribution (e.g. coincident with the most recent period of separation ~15 kya; Meyers et al., 1998). Our ENMs for *L. rufus* and *L. macrotis-L. millsoni* suggested the exposed land bridge was climatically suitable for both lineages during the Last Glacial Maximum (~21 kya). Thus, it is surprising that only *L. rufus* is known to occur on the island despite the more expansive geographic distribution and greater environmental breadth of the *L. macrotis-L. millsoni* lineage. The absence of *L. millsoni* on Bioko may be a result of differences in breeding biology between the species given the absence of slow-moving rivers on the island (the preferred breeding sites of *L. millsoni*) versus the ready abundance of small, fast flowing streams (the preferred breeding sites of *L. rufus*; Amiet & Schiøtz, 1974). The amphibian fauna of Bioko is still incompletely known, however, and two other widespread species of *Leptopelis* (*L. notatus* and *L. ocellatus*) occur

throughout the Atlantic Equatorial Forest, but have not yet been reported from Bioko Island (Sánchez-Vialas et al., 2020). Thus, it is possible that *L. millsoni* occurs on Bioko and has not yet been detected or has been misidentified as *L. rufus*. Phylogeographic studies of other large-bodied Bioko anurans including forest tree frogs (Bell et al., 2019), foam-nesting tree frogs (Leaché et al., 2019), white-lipped frogs (Jongsma et al., 2018), and clawed frogs (Evans et al., 2015) found very little genetic differentiation between island and continental populations. By contrast, phylogeographic studies of smaller-bodied anurans including leaf-folding frogs (Charles et al., 2018) and reed frogs (Bell et al., 2017) found modest genetic differentiation. This pattern suggests that species-specific traits, such as reproductive biology and dispersal ability, result in different responses to a shared landscape feature (e.g. Papadopoulou & Knowles, 2015).

4.4 | Biogeographic barriers, climatic stability, and isolation by environment in *L. macrotis* and *L. millsoni*

The history of intraspecific divergence in *L. macrotis* and *L. millsoni* appears to be relatively complex with a combination of biogeographic barriers, Quaternary refugia, and ecological gradients contributing to lineage divergence. For instance, we found distinct lineages of *L. millsoni* on either side of the Sanaga and Congo Rivers, and both rivers coincide with intra- and interspecific levels of divergence in a range of taxa including the ground dwelling long-fingered frogs (Hirschfeld et al., 2015), swamp rats (Bohoussou et al., 2015), arboreal snakes (Allen et al., 2021), and chimpanzees (Hey, 2010). Likewise, our ENMs identify several regions within West and Central African rainforests as climatically suitable throughout the late Pleistocene to present day for *L. macrotis* and *L. millsoni*, and these regions overlap with refugia proposed by previous authors (Maley, 1996). These centres of stability also closely corresponded with population genetic structure, with the exception of relict populations in the last remaining forest fragments in Angola (Ernst et al., 2020). Furthermore, intraspecific divergence times within *L. macrotis* and *L. millsoni* indicated that lineage formation occurred during the Pleistocene, which is temporally consistent with isolation in climatic refugia and intraspecific divergence in other codistributed species (Bell et al., 2017; Bohoussou et al., 2015; Jacquet et al., 2015; Leaché et al., 2019). We found that population genetic structure within *L. macrotis* and *L. millsoni* was associated with both geographic distance and climatic variables (annual precipitation and mean diurnal range in temperature for *L. millsoni* and *L. macrotis*, respectively), suggesting that reduced dispersal and local adaptation both play a role in structuring populations across West and Central Africa. Similar patterns have been observed in other Central African rainforest species including trees (Helmstetter, Béthune, et al., 2020) and duikers (Ntie et al., 2017).

Differentiating between riverine barriers, climatic refugia, and ecological gradients based solely on phylogeographic patterns can be challenging when these features overlap geographically (Portik et al., 2017). Our small sample sizes for several key populations

precluded explicitly testing between alternative divergence scenarios within *L. macrotis* and *L. millsoni*, as well as range expansion of *L. millsoni* into Central Africa. For example, we found distinct lineages of *L. millsoni* on either side of the Sanaga River, yet this entire region is within a region of historically suitable climate. As additional samples become available through increased fieldwork, specific tests of range expansion and alternative demographic models accounting for divergence time, gene flow, and population size can be used to differentiate between the historical processes that produced genetically distinct populations within *L. millsoni* and *L. macrotis*. In addition, genome scans and identification of correlations between allele frequencies and local environmental variation would further clarify the role of ecological gradients and local adaptation in population divergence (e.g. Morgan et al., 2020; Zhen et al., 2017).

ACKNOWLEDGEMENTS

For fieldwork we thank: Centre National de la Recherche Scientifique et Technologique, Agence Nationale des Parcs Nationaux, and the Direction de la Faune et des Aires Protégées for permits, the Wildlife Conservation Society for logistical support, and field companions T. Essone, B. Hylayre, P. Minko, F. Moiniyoko (Gabon); Universidad Nacional de Guinea Equatorial and J. M. Esara Echube for permits, the Bioko Biodiversity Protection Program, ExxonMobil Foundation, and Mobil Equatorial Guinea Inc. for logistical support (Equatorial Guinea); Management of Nigerian National Park Service for permits (NPH/GEN/121/XXV/461) and field companion R. Oluchukwu Mbatugosi (Nigeria); Ministère des Forêts et de la Faune and Ministère de la Recherche Scientifique et de l'Innovation for permits, Congo Basin Institute for logistical support, and field companions D. Fotibu, B. Freiermuth, L. Scheinberg, R. Tarvin (Cameroon); Instituto Nacional da Biodiversidade e Áreas de Conservação, Ministério do Ambiente, República de Angola and the Gabinete Provincial da Agricultura, Pecuária e Pescas do Uíge for permits (122/INBAC. MINAMB/2013, no. 17/014, no. 02/018; no. 05/2019), M.F. Branquima, J. Lau, T. Lautenschläger, and the University of Kimpa Vita, Uíge for logistical support (Angola); Centre de Recherche en Sciences Naturelles and Institut Congolais pour la Conservation de la Nature for permits, and field companions Mwenebatu M. Aristote and Wandegé M. Muninga (Democratic Republic of Congo); Forestry Development Authority of the Republic of Liberia for permits (Ref: MD/037/2018/11) and the Wild Chimpanzee Foundation and the Society for the Conservation of Nature of Liberia for logistical support (Liberia); and Ministère de l'Enseignement Supérieur et de la Recherche Scientifique for permits (Côte d'Ivoire). Genetic data collection was funded by the National Science Foundation (NSF) awards DEB-1456098 (A.D.L) and DEB-1457232 (M.K.F.), a Smithsonian National Museum of Natural History (NMNH) Research Grant (R.C.B.), and Fundação para a Ciência e Tecnologia (FCT) UIDB/50027/2020 (N.L.B.). K.E.J. was supported by the NMNH Natural History Research Experience REU program (NSF-OCE:1560088). E.A.M. was supported by an NMNH Peter Buck and Rathbone Bacon Fellowship. N.L.B. was supported by FCT SFRH/

PD/BD/140810/2018. R.E. was supported by the German Academic Exchange Service (DAAD). G.F.M.J. was supported by an NSERC fellowship (PGSD2/516563-2018). Fieldwork was funded by the National Geographic Society award no. 8556-08 (E.G.), the NSF (DEB-1145459, E.G.; DEB-1202609, D.C.B.), the DFG VE 183/4-1 & RO 3064/1-2 (M.O.R.), BMBF-Project W08 BIOTA-West, 01LC0017 (M.O.R.), Conservation International (M.O.R.), the Critical Ecosystem Partnership Fund (M.O.R.), the Declining Amphibian Population Task Force (M.O.R.), the Czech Science Foundation GACR 15-13415Y (V.G.), the Ministry of Culture of the Czech Republic DKRVO 2019–2023/6.VII.c, National Museum, 00023272 (V.G.), and the Ministério do Ambiente - Instituto Nacional da Biodiversidade e Áreas de Conservação (INBAC). Specimens borrowed from BYU were collected with funding from NSF award EF-1241885. We thank L. Scheinberg, J. Vindum, C. Spencer, J. Rosado, J. Sites for providing access to specimens and J. Streicher at NHM, London for graciously measuring type specimens of *L. millsoni*. We thank T. J. Finerno for assisting with ddRADseq data collection, M. Jirků, D. Modrý and M. Dolinay for providing additional material for study, and Bryan Carstens and two anonymous reviewers for thoughtful suggestions during peer review. Portions of the laboratory and computer work were conducted in and with the support of the L.A.B. facilities of the NMNH. This is Smithsonian Institution, Gabon Biodiversity Programme contribution number 201.

AUTHOR CONTRIBUTIONS

Rayna C. Bell designed the project; Jeannot B. Akuboy, Gabriel Badjedjea, Abraham Bamba-Kaya, Ninda L. Baptista, Rayna C. Bell, David C. Blackburn, Raffael Ernst, Eli Greenbaum, Václav Gvoždík, Gregory F. M. Jongsma, Marcel T. Kouete, Chifundera Kusamba, Adam D. Leaché, Franck M. Masudi, Patrick J. McLaughlin, Lotanna M. Nneji, Abiodun B. Onadeko, Johannes Penner, Pedro Vaz Pinto, Daniel M. Portik, Mark-Oliver Rödel, Bryan L. Stuart, Elie Tobi, Ange-Ghislain Zassi-Boulou collected field samples and contributed funding for fieldwork; Ninda L. Baptista, Rayna C. Bell, David C. Blackburn, Raffael Ernst, Eli Greenbaum, Václav Gvoždík, Kyle E. Jaynes, Gregory F. M. Jongsma, Lotanna M. Nneji, Mark-Oliver Rödel, Elie Tobi collected data; Rayna C. Bell, Kyle E. Jaynes, Edward A. Myers analysed the data; Rayna C. Bell, Adam D. Leaché, Matthew K. Fujita contributed funding for data collection; Rayna C. Bell, Kyle E. Jaynes, Edward A. Myers wrote the manuscript with input from all authors.

DATA AVAILABILITY STATEMENT

DNA sequences: GenBank accession numbers MZ348238–MZ348246; MZ348354–MZ348357; MZ408684–MZ408793; MZ408795–MZ408888; MZ496581–MZ496587 and SRA accession numbers SAMN21218886–SAMN21219053 in Table S1.

Sampling localities and voucher information for molecular data analyses and environmental niche models in Table S1). Morphological measurements in Table S2). Scripts for demographic modeling and environmental niche modeling at <https://github.com/eddiemyers/Leptopelis>.

ORCID

- Kyle E. Jaynes  <https://orcid.org/0000-0002-4188-0468>
- Edward A. Myers  <https://orcid.org/0000-0001-5369-6329>
- Václav Gvoždík  <https://orcid.org/0000-0002-4398-4076>
- David C. Blackburn  <https://orcid.org/0000-0002-1810-9886>
- Daniel M. Portik  <https://orcid.org/0000-0003-3518-7277>
- Eli Greenbaum  <https://orcid.org/0000-0003-1674-1316>
- Gregory F. M. Jongsma  <https://orcid.org/0000-0001-8790-2610>
- Raffael Ernst  <https://orcid.org/0000-0001-6347-1414>
- Franck M. Masudi  <https://orcid.org/0000-0002-3600-173X>
- Patrick J. McLaughlin  <https://orcid.org/0000-0002-3383-8999>
- Lotanna M. Nneji  <https://orcid.org/0000-0003-1422-1683>
- Abiodun B. Onadeko  <https://orcid.org/0000-0002-0430-5026>
- Johannes Penner  <https://orcid.org/0000-0001-8166-5992>
- Pedro Vaz Pinto  <https://orcid.org/0000-0003-4487-1310>
- Bryan L. Stuart  <https://orcid.org/0000-0003-4719-1951>
- Adam D. Leaché  <https://orcid.org/0000-0001-8929-6300>
- Matthew K. Fujita  <https://orcid.org/0000-0002-5179-7801>
- Rayna C. Bell  <https://orcid.org/0000-0002-0123-8833>

REFERENCES

- Ahl, E. (1929). Zur Kenntnis der afrikanischen Baumfrosch-Gattung *Leptopelis*. *Sitzungsberichte Der Gesellschaft Naturforschender Freunde Zu Berlin*, 1929, 185–222.
- Ahl, E. (1931). Anura III, Polypedatidae. *Das Tierreich*, 55, 1–477.
- Aiello-Lammens, M. E., Boria, R. A., Radosavljevic, A., Vilela, B., & Anderson, R. P. (2015). spThin: An R package for spatial thinning of species occurrence records for use in ecological niche models. *Ecography*, 38(5), 541–545. <https://doi.org/10.1111/ecog.01132>
- Allen, K. E., Greenbaum, E., Hime, P. M., Tapondjou N., W. P., Sterkhova, V. V., Kusamba, C., Rödel, M.-O., Penner, J., Peterson, A. T., & Brown, R. M. (2021). Rivers, not refugia, drove diversification in arboreal, sub-Saharan African snakes. *Ecology and Evolution*, 11, 6133–6152. <https://doi.org/10.1002/ece3.7429>
- Amiet, J. L. (2012). Les Rainettes du Cameroun (Amphibiens Anoures). *Nyons & Saint Nazaire*, Édition J.-L. Amiet & La Nef des Livres.
- Amiet, J.-L., & Goutte, S. (2017). Chants d'Amphibiens du Cameroun. *Nyons & Saint Nazaire*, J.-L. Amiet & Éditions Petit Génie.
- Amiet, J.-L., & Schiøtz, A. (1974). Voix d'Amphibiens camerounais III. Hyperoliidae: genre *Leptopelis*. *Annales De La Faculté Des Sciences Du Cameroun*, 17, 131–163.
- Bell, R. C., McLaughlin, P. J., Jongsma, G. F. M., Blackburn, D. C., & Stuart, B. L. (2019). Morphological and genetic variation of *Leptopelis brevirostris* encompasses the little-known treefrogs *Leptopelis crystallinoron* from Gabon and *Leptopelis brevipes* from Bioko Island. *Equatorial Guinea. African Journal of Herpetology*, 68(2), 91–117.
- Bell, R. C., Parra, J. L., Badjedjea, G., Barej, M. F., Blackburn, D. C., Burger, M., Channing, A., Dehling, J. M., Greenbaum, E., Gvoždík, V., Kielgast, J., Kusamba, C., Lötters, S., McLaughlin, P. J., Nagy, Z. T., Rödel, M.-O., Portik, D. M., Stuart, B. L., VanDerWal, J., ... Zamudio, K. R. (2017). Idiosyncratic responses to climate-driven forest fragmentation and marine incursions in reed frogs from Central Africa and the Gulf of Guinea Islands. *Molecular Ecology*, 26(19), 5223–5244. <https://doi.org/10.1111/mec.14260>
- Bohoussou, K. H., Cornette, R., Akpatou, B., Colyn, M., Peterhans, J. K., Kennis, J., & Nicolas, V. (2015). The phylogeography of the rodent genus *Malacomys* suggests multiple Afrotropical Pleistocene lowland forest refugia. *Journal of Biogeography*, 42(11), 2049–2061.
- Bolger, A. M., Lohse, M., & Usadel, B. (2014). Trimmomatic: A flexible trimmer for Illumina Sequence Data. *Bioinformatics*, 30(15), 2114–2120. <https://doi.org/10.1093/bioinformatics/btu170>
- Bonnefille, R. (2010). Cenozoic vegetation, climate changes, and hominid evolution in tropical Africa. *Global and Planetary Change*, 72(4), 390–411. <https://doi.org/10.1016/j.gloplacha.2010.01.015>
- Booth, A. H. (1958). The Niger, the Volta, and the Dahomey Gap as geographic barriers. *Evolution*, 12(1), 48–62. <https://doi.org/10.1111/j.1558-5646.1958.tb02927.x>
- Bouckaert, R., Heled, J., Kühnert, D., Vaughan, T., Wu, C.-H., Xie, D., Suchard, M. A., Rambaut, A., & Drummond, A. J. (2014). BEAST 2: A software platform for Bayesian evolutionary analysis. *PLoS Biology*, 10(4), e1003537. <https://doi.org/10.1371/journal.pcbi.1003537>
- Boul, K. E., Funk, C. W., Darst, C. R., Cannatella, D. C., & Ryan, M. J. (2006). Sexual selection drives speciation in an Amazonian frog. *Proceedings of the Royal Society B: Biological Sciences*, 274(1608), 399–406.
- Broennimann, O., Fitzpatrick, M. C., Pearman, P. B., Petitpierre, B., Pellissier, L., Yoccoz, N. G., Thuiller, W., Fortin, M.-J., Randin, C., Zimmermann, N. E., Graham, C. H., & Guisan, A. (2012). Measuring ecological niche overlap from occurrence and spatial environmental data. *Global Ecology and Biogeography*, 21(4), 481–497. <https://doi.org/10.1111/j.1466-8238.2011.00698.x>
- Bryant, D., Bouckaert, R., Felsenstein, J., Rosenberg, N. A., & RoyChoudhury, A. (2012). Inferring species trees directly from biallelic genetic markers: bypassing gene trees in a full coalescent analysis. *Molecular Biology and Evolution*, 29(8), 1917–1932. <https://doi.org/10.1093/molbev/mss086>
- Channing, A., & Rödel, M. O. (2019). *Field guide to the frogs and other amphibians of Africa*. Struik Nature.
- Charles, K. L., Bell, R. C., Blackburn, D. C., Burger, M., Fujita, M. K., Gvoždík, V., Jongsma, G. F. M., Kouete, M. T., Leaché, A. D., & Portik, D. M. (2018). Sky, sea, and forest islands: Diversification in the African leaf-folding frog *Afraxalus paradorsalis* (Anura: Hyperoliidae) of the Lower Guineo-Congolian rain forest. *Journal of Biogeography*, 45(8), 1781–1794. <https://doi.org/10.1111/jbi.13365>
- Couvreur, T. L. P., Dauby, G., Blach-Overgaard, A., Deblauwe, V., Dessein, S., Droissart, V., Hardy, O. J., Harris, D. J., Janssens, S. B., Ley, A. C., Mackinder, B. A., Sonké, B., Sosef, M. S. M., Stévant, T., Svenning, J.-C., Wieringa, J. J., Faye, A., Missoup, A. D., Tolley, K. A., ... Sepulchre, P. (2021). Tectonics, climate and the diversification of the tropical African terrestrial flora and fauna. *Biological Reviews*, 96, 16–51. <https://doi.org/10.1111/brv.12644>
- Danecek, P., Auton, A., Abecasis, G., Albers, C. A., Banks, E., DePristo, M. A., Handsaker, R. E., Lunter, G., Marth, G. T., Sherry, S. T., McVean, G., & Durbin, R. (2011). The variant call format and VCFtools. *Bioinformatics*, 27(15), 2156–2158. <https://doi.org/10.1093/bioinformatics/btr330>
- Darriba, D., Taboada, G. L., Doallo, R., & Posada, D. (2012). jModelTest 2: more models, new heuristics and parallel computing. *Nature Methods*, 9(8), 772. <https://doi.org/10.1038/nmeth.2109>
- de Medeiros, B. A. (2019) Matrix Condenser v.1.0. Available at: https://github.com/brunoasm/matrix_condenser/
- Drummond, A. J., Suchard, M. A., Xie, D., & Rambaut, A. (2012). Bayesian phylogenetics with BEAUti and the BEAST 1.7. *Molecular Biology and Evolution*, 29(8), 1969–1973. <https://doi.org/10.1093/molbev/mss075>
- Dupont, L. M., Jahns, S., Marret, F., & Ning, S. (2000). Vegetation change in equatorial West Africa: time-slices for the last 150 ka. *Palaeogeography, Palaeoclimatology, Palaeoecology*, 155(1–2), 95–122. [https://doi.org/10.1016/S0031-0182\(99\)00095-4](https://doi.org/10.1016/S0031-0182(99)00095-4)
- Ernst, R., Lautenschläger, T., Branquima, M. F., & Hölting, M. (2020). At the edge of extinction: a first herpetological assessment of the proposed Serra do Pingano Rainforest National Park in Uíge Province, northern Angola. *Zoosystematics and Evolution*, 96(1), 237–262. <https://doi.org/10.3897/zse.96.51997>

- Evans, B. J., Carter, T. F., Greenbaum, E., Gvoždik, V., Kelley, D. B., McLaughlin, P. J., Pauwels, O. S. G., Portik, D. M., Stanley, E. L., Tinsley, R. C., Tobias, M. L., & Blackburn, D. C. (2015). Genetics, morphology, advertisement calls, and historical records distinguish six new polyploid species of African Clawed Frog (*Xenopus*, Pipidae) from West and Central Africa. *PLoS One*, *10*(12), e0142823. <https://doi.org/10.1371/journal.pone.0142823>
- Excoffier, L., Dupanloup, I., Huerta-Sánchez, E., Sousa, V. C., & Foll, M. (2013). Robust demographic inference from genomic and SNP data. *PLoS Genetics*, *9*(10), e1003905. <https://doi.org/10.1371/journal.pgen.1003905>
- Ferrier, S., Manion, G., Elith, J., & Richardson, K. (2007). Using generalized dissimilarity modelling to analyse and predict patterns of beta diversity in regional biodiversity assessment. *Diversity and Distributions*, *13*(3), 252–264. <https://doi.org/10.1111/j.1472-4642.2007.00341.x>
- Fitzpatrick, B. M., Fordyce, J. A., & Gavrilets, S. (2009). Pattern, process, and geographic modes of speciation. *Journal of Evolutionary Biology*, *22*, 2342–2347. <https://doi.org/10.1111/j.1420-9101.2009.01833.x>
- Fox, J. H. (1995). Morphological correlates of auditory sensitivity in anuran amphibians. *Brain, Behavior and Evolution*, *45*(6), 327–338. <https://doi.org/10.1159/000113560>
- Freeman, E. A., & Moisen, G. G. (2008). A comparison of the performance of threshold criteria for binary classification in terms of predicted prevalence and kappa. *Ecological Modelling*, *217*(1–2), 48–58. <https://doi.org/10.1016/j.ecolmodel.2008.05.015>
- Frichot, E., & François, O. (2015). LEA: An R package for landscape and ecological association studies. *Methods in Ecology and Evolution*, *6*(8), 925–929. <https://doi.org/10.1111/2041-210X.12382>
- Frichot, E., Mathieu, F., Trouillon, T., Bouchard, G., & François, O. (2014). Fast and efficient estimation of individual ancestry coefficients. *Genetics*, *196*(4), 973–983. <https://doi.org/10.1534/genetics.113.160572>
- Friis, G., & Milá, B. (2020). Change in sexual signalling traits outruns morphological divergence across an ecological gradient in the post-glacial radiation of the songbird genus *Junco*. *Journal of Evolutionary Biology*, *33*(9), 1276–1293.
- Gaubert, P., Antunes, A., Meng, H., Miao, L., Peigné, S., Justy, F., Njikou, F., Dufour, S., Danquah, E., Alahakoon, J., Verheyen, E., Stanley, W. T., O'Brien, S. J., Johnson, W. E., & Luo, S.-J. (2018). The complete phylogeny of Pangolins: Scaling up resources for the molecular tracing of the most trafficked mammals on Earth. *Journal of Heredity*, *109*(4), 347–359. <https://doi.org/10.1093/jhered/esx097>
- Gingras, B., Boeckle, M., Herbst, C. T., & Fitch, W. T. (2013). Call acoustics reflect body size across four clades of anurans. *Journal of Zoology*, *289*, 143–150. <https://doi.org/10.1111/j.1469-7998.2012.00973.x>
- Goudie, A. S. (2005). The drainage of Africa since the cretaceous. *Geomorphology*, *67*, 437–456. <https://doi.org/10.1016/j.geomorph.2004.11.008>
- Hardy, O. J., Born, C., Budde, K., Daïnou, K., Dauby, G., Duminil, J., Ewédjé, E.-E., Gomez, C., Heuertz, M., Koffi, G. K., Lowe, A. J., Micheneau, C., Ndiade-Bouroubo, D., Piñeiro, R., & Poncet, V. (2013). Comparative phylogeography of African rain forest trees: a review of genetic signatures of vegetation history in the Guineo-Congolian region. *Comptes Rendus GeoScience*, *345*, 284–296. <https://doi.org/10.1016/j.crte.2013.05.001>
- Hassanin, A., Khouider, S., Gembu, G.-C., M. Goodman, S., Kadjo, B., Nesi, N., Pourrut, X., Nakouné, E., & Bonillo, C. (2015). The comparative phylogeography of fruit bats of the tribe Scotonycterini (Chiroptera, Pteropodidae) reveals cryptic species diversity related to African Pleistocene forest refugia. *Comptes Rendus Biologies*, *338*(3), 197–211. <https://doi.org/10.1016/j.crvi.2014.12.003>
- Helmstetter, A. J., Amoussou, B. E. N., Béthune, K., Kamdem, N. G., Glélé Kaki, R., Sonké, B., & Couvreur, T. L. P. (2020). Phylogenomic approaches reveal how climate shapes patterns of genetic diversity in an African rain forest tree species. *Molecular Ecology*, *29*(18), 3560–3573. <https://doi.org/10.1111/mec.15572>
- Helmstetter, A. J., Béthune, K., Kamdem, N. G., Sonké, B., & Couvreur, T. L. P. (2020). Individualistic evolutionary responses of central African rain forest plants to Pleistocene climatic fluctuations. *Proceedings of the National Academy of Sciences, USA*, *117*(5), 32509–32518. <https://doi.org/10.1073/pnas.2001018117>
- Hetherington, T. E. (1994). Sexual differences in the tympanic frequency responses of the American bullfrog (*Rana catesbeiana*). *Journal of the Acoustical Society of America*, *96*, 1186–1188.
- Heuertz, M., Duminil, J., Dauby, G., Savolainen, V., & Hardy, O. J. (2014). Comparative phylogeography in rainforest trees from Lower Guinea. *PLoS One*, *9*, e84307.
- Hey, J. (2010). The divergence of chimpanzee species and subspecies as revealed in multipopulation isolation-with-migration analyses. *Molecular Biology and Evolution*, *27*(4), 921–933. <https://doi.org/10.1093/molbev/msp298>
- Hijmans, R. J., Cameron, S. E., Parra, J. L., Jones, P. G., & Jarvis, A. (2005). Very high resolution interpolated climate surfaces for global land areas. *International Journal of Climatology*, *25*(15), 1965–1978. <https://doi.org/10.1002/joc.1276>
- Hirschfeld, M., Blackburn, D. C., Burger, M., Greenbaum, E., Zassi-Boulou, A.-G., & Rödel, M.-O. (2015). Two new species of long-fingered frogs of the genus *Cardioglossa* (Anura: Arthroleptidae) from Central African rainforests. *African Journal of Herpetology*, *64*(2), 81–102.
- Hoskin, C. J., James, S., & Grigg, G. C. (2009). Ecology and taxonomy-driven deviations in the frog call-body size relationship across the diverse Australian frog fauna. *Journal of Zoology*, *278*, 36–41. <https://doi.org/10.1111/j.1469-7998.2009.00550.x>
- Huntley, J. W., & Voelker, G. (2016). Cryptic diversity in Afro-tropical lowland forests: The systematics and biogeography of the avian genus *Bleda*. *Molecular Phylogenetics and Evolution*, *99*, 297–308. <https://doi.org/10.1016/j.ympev.2016.04.002>
- Jacquet, F., Denys, C., Verheyen, E., Bryja, J., Hutterer, R., Kerbis Peterhans, J. C., Stanley, W. T., Goodman, S. M., Couloux, A., Colyn, M., & Nicolas, V. (2015). Phylogeography and evolutionary history of the *Crocidura olivieri* complex (Mammalia, Soricomorpha): from a forest origin to broad ecological expansion across Africa. *BMC Evolutionary Biology*, *15*, 71. <https://doi.org/10.1186/s12862-015-0344-y>
- Jaynes, K. E., Myers, E. A., Drewes, R. C., & Bell, R. C. (2021). New evidence for distinctiveness of the island-endemic Principe Giant Tree Frog (Arthroleptidae: *Leptopelis palmatus*). *Herpetological Journal*, *31*(3), 162–169. <https://doi.org/10.33256/31.3.162169>
- Jombart, T. (2008). ADEGENET: a R package for the multivariate analysis of genetic markers. *Bioinformatics*, *24*(11), 1403–1405. <https://doi.org/10.1093/bioinformatics/btn129>
- Jombart, T., Devillard, S., & Balloux, F. (2010). Discriminant analysis of principal components: a new method for the analysis of genetically structured populations. *BMC Genetics*, *11*, 94. <https://doi.org/10.1186/1471-2156-11-94>
- Jongsma, G. F. M., Barej, M. F., Barratt, C. D., Burger, M., Conradie, W., Ernst, R., Greenbaum, E., Hirschfeld, M., Leaché, A. D., Penner, J., Portik, D. M., Zassi-Boulou, A.-G., Rödel, M.-O., & Blackburn, D. C. (2018). Diversity and biogeography of frogs in the genus *Amnirana* (Anura: Ranidae) across sub-Saharan Africa. *Molecular Phylogenetics and Evolution*, *120*, 274–285. <https://doi.org/10.1016/j.ympev.2017.12.006>
- Katoh, K., Misawa, K., Kuma, K.-I., & Miyata, T. (2002). MAFFT: a novel method for rapid multiple sequence alignment based on fast Fourier transform. *Nucleic Acids Research*, *30*(14), 3059–3066. <https://doi.org/10.1093/nar/gkf436>
- Katoh, K., & Standley, D. M. (2013). MAFFT Multiple Sequence Alignment Software version 7: improvements in performance and

- usability. *Molecular Biology and Evolution*, 30(4), 772–780. <https://doi.org/10.1093/molbev/mst010>
- Koenen, E. J., Clarkson, J. J., Pennington, T. D., & Chatrou, L. W. (2015). Recently evolved diversity and convergent radiations of rainforest mahoganies (Meliaceae) shed new light on the origins of rainforest hyperdiversity. *New Phytologist*, 207, 327–339. <https://doi.org/10.1111/nph.13490>
- Krishnan, A., & Tamma, K. (2016). Divergent morphological and acoustic traits in sympatric communities of Asian barbets. *Royal Society of Open Science*, 3, 160117. <https://doi.org/10.1098/rsos.160117>
- Lattenkamp, E. Z., Nagy, M., Drexler, M., Vernes, S. C., Wiegrebbe, L., & Knörnschild, M. (2021). Hearing sensitivity and amplitude coding in bats are differentially shaped by echolocation calls and social calls. *Proceedings Royal Society B: Biological Sciences*, 288, 20202600.
- Leaché, A. D., Portik, D. M., Rivera, D., Rödel, M.-O., Penner, J., Gvoždík, V., Greenbaum, E., Jongsma, G. F. M., Ofori-Boateng, C., Burger, M., Eniang, E. A., Bell, R. C., & Fujita, M. K. (2019). Exploring rain forest diversification using demographic model testing in the African foam-nest treefrog *Chiromantis rufescens*. *Journal of Biogeography*, 46(12), 2706–2721. <https://doi.org/10.1111/jbi.13716>
- Linck, E., & Battey, C. J. (2019). Minor allele frequency thresholds strongly affect population structure inference with genomic data sets. *Molecular Ecology Resources*, 19(3), 639–647. <https://doi.org/10.1111/1755-0998.12995>
- Lynch, M. (2010). Rate, molecular spectrum, and consequences of human mutation. *Proceedings of the National Academy of Sciences, USA*, 107(3), 961–968. <https://doi.org/10.1073/pnas.0912629107>
- Maley, J. (1996). The African rainforest: main characteristics of changes in vegetation and climate from the Upper-Cretaceous to the Quaternary. *Proceedings of the Royal Society of Edinburgh B: Biological Sciences*, 104, 31–73.
- Manion, G., Lisk, M., Ferrier, S., Nieto-Lugilde, D., & Fitzpatrick, M. C. (2016). gdm: Functions for generalized dissimilarity modeling. R package Version, 1, No. 7.
- Marshall, C. A. M., Wieringa, J. J., & Hawthorne, W. D. (2021). An interpolated biogeographical framework for tropical Africa using plant species distributions and the physical environment. *Journal of Biogeography*, 48, 23–36. <https://doi.org/10.1111/jbi.13976>
- Marzoli, A., Piccirillo, E. M., Renne, P. R., Bellieni, G., Iacumin, M., Nyobe, J. B., & Tongwa, A. T. (2000). The Cameroon volcanic line revisited: Petrogenesis of continental basaltic magmas from lithospheric and Asthenospheric mantle sources. *Journal of Petrology*, 41, 87–109. <https://doi.org/10.1093/petrology/41.1.87>
- Mayr, E. (1942). *Systematics and the Origin of Species*. Columbia University Press.
- Meyers, J. B., Rosendahl, B. R., Harrison, C. G., & Ding, Z.-D. (1998). Deep-imaging seismic and gravity results from the offshore Cameroon Volcanic Line, and speculation of African hotlines. *Tectonophysics*, 284, 31–63. [https://doi.org/10.1016/S0040-1951\(97\)00173-X](https://doi.org/10.1016/S0040-1951(97)00173-X)
- Morgan, K., Mboumba, J.-F., Ntie, S., Mickala, P., Miller, C. A., Zhen, Y., & Anthony, N. M. (2020). Precipitation and vegetation shape patterns of genomic and craniometric variation in the central African rodent *Praomys misonnei*. *Proceedings of the Royal Society B: Biological Sciences*, 287, 20200449.
- Morley, R. J. (2000). *Origin and evolution of tropical rain forests*. John Wiley and Sons.
- Muscarella, R., Galante, P. J., Soley-Guardia, M., Boria, R. A., Kass, J. M., Uriarte, M., & Anderson, R. P. (2014). ENM eval: An R package for conducting spatially independent evaluations and estimating optimal model complexity for Maxent ecological niche models. *Methods in Ecology and Evolution*, 5(11), 1198–1205.
- Myers, E. A., McKelvy, A. D., & Burbrink, F. T. (2020). Biogeographic barriers, Pleistocene refugia, and climatic gradients in the south-eastern Nearctic drive diversification in cornsnakes (*Pantherophis guttatus* complex). *Molecular Ecology*, 29(4), 797–811.
- Myers, N., Mittermeier, R. A., Mittermeier, C. G., Da Fonseca, G. A., & Kent, J. (2000). Biodiversity hotspots for conservation priorities. *Nature*, 403(6772), 853–858.
- Nei, M. (1972). Genetic distance between populations. *American Naturalist*, 106(949), 283–292. <https://doi.org/10.1086/282771>
- Nicolas, V., Fabre, P.-H., Bryja, J., Denys, C., Verheyen, E., Missouf, A. D., Olayemi, A., Katuala, P., Dudu, A., Colyn, M., Kerbis Peterhans, J., & Demos, T. (2020). The phylogeny of the African wood mice (Muridae, *Hylomyscus*) based on complete mitochondrial genomes and five nuclear genes reveals their evolutionary history and undescribed diversity. *Molecular Phylogenetics and Evolution*, 144, 106703. <https://doi.org/10.1016/j.ympev.2019.106703>
- Njabo, K. Y., Bowie, R. C. K., & Sorenson, M. D. (2008). Phylogeny, biogeography and taxonomy of the African wattle-eyes (Aves: Passeriformes: Platysteiridae). *Molecular Phylogenetics and Evolution*, 48, 136–149. <https://doi.org/10.1016/j.ympev.2008.01.013>
- Noble, G. K. (1924). Contributions of the herpetology of the Belgian Congo based on the collection of the American Museum Congo Expedition, 1909–1915. Part 3, Amphibia. *Bulletin of the American Museum of Natural History*, 49, 147–347.
- Ntie, S., Davis, A. R., Hils, K., Mickala, P., Thomassen, H. A., Morgan, K., Vanthomme, H., Gonder, M. K., & Anthony, N. M. (2017). Evaluating the role of Pleistocene refugia, rivers and environmental variation in the diversification of central African duikers (genera *Cephalophus* and *Philantomba*). *BMC Evolutionary Biology*, 17, 212. <https://doi.org/10.1186/s12862-017-1054-4>
- Olson, D. M., Dinerstein, E., Wikramanayake, E. D., Burgess, N. D., Powell, G. V. N., Underwood, E. C., D'Amico, J. A., Itoua, I., Strand, H. E., Morrison, J. C., Loucks, C. J., Allnutt, T. F., Ricketts, T. H., Kura, Y., Lamoreux, J. F., Wettengel, W. W., Hedao, P., & Kassem, K. R. (2001). Terrestrial ecoregions of the world: A new map of life on Earth. *BioScience*, 51, 933–938.
- Ortiz, E. M. (2019). vcf2phyloip v2.0: convert a VCF matrix into several matrix formats for phylogenetic analysis. <https://doi.org/10.5281/zenodo.2540861>
- Palumbi, S., Martin, A., Roman, S., McMillan, W. O., Stice, L., & Grabowski, G. (1991). *The simple fool's guide to PCR. Version 2*. University of Hawaii, Honolulu.
- Papadopoulou, A., & Knowles, L. L. (2015). Species-specific responses to island connectivity cycles: Refined models for testing phylogeographic concordance across a Mediterranean Pleistocene Aggregate Island Complex. *Molecular Ecology*, 24(16), 4252–4268.
- Penner, J., Wegmann, M., Hillers, A., Schmidt, M., & Rödel, M.-O. (2011). A hotspot revisited – a biogeographical analysis of West African amphibians. *Diversity and Distributions*, 17, 1077–1088. <https://doi.org/10.1111/j.1472-4642.2011.00801.x>
- Perret, J.-L. (1973). *Leptopelis palmatus* et *Leptopelis rufus*, deux espèces distinctes. *Annales De La Faculté Des Sciences Du Yaoundé*, 15–16, 81–90.
- Peterson, B. K., Weber, J. N., Kay, E. H., Fisher, H. S., & Hoekstra, H. E. (2012). Double digest RADseq: an inexpensive method for *De Novo* SNP discovery and genotyping in model and non-model species. *PLoS One*, 7(5), e37135. <https://doi.org/10.1371/journal.pone.0037135>
- Phillips, S. J., Anderson, R. P., & Schapire, R. E. (2006). Maximum entropy modeling of species geographic distributions. *Ecological Modelling*, 190(3–4), 231–259. <https://doi.org/10.1016/j.ecolmod.2005.03.026>
- Pigot, A. L., & Tobias, J. A. (2015). Dispersal and the transition to sympatry in vertebrates. *Proceedings of the Royal Society B: Biological Sciences*, 282, 20141929.
- Portik, D. M., Bell, R. C., Blackburn, D. C., Bauer, A. M., Barratt, C. D., Branch, W. R., Burger, M., Channing, A., Colston, T. J., Conradie, W., Dehling, J. M., Drewes, R. C., Ernst, R., Greenbaum, E., Gvoždík, V., Harvey, J., Hillers, A., Hirschfeld, M., Jongsma, G. F. M., ... McGuire, J. A. (2019). Sexual dichromatism drives diversification within a

- major radiation of African amphibians. *Systematic Biology*, 68(6), 859–875. <https://doi.org/10.1093/sysbio/syz023>
- Portik, D. M., Leaché, A. D., Rivera, D., Barej, M. F., Burger, M., Hirschfeld, M., Rödel, M.-O., Blackburn, D. C., & Fujita, M. K. (2017). Evaluating mechanisms of diversification in a Guineo-Congolian tropical forest frog using demographic model selection. *Molecular Ecology*, 26(19), 5245–5263. <https://doi.org/10.1111/mec.14266>
- Portillo, F., & Greenbaum, E. (2014a). A new species of the *Leptopelis modestus* complex (Anura: Arthroleptidae) from the Albertine Rift of Central Africa. *Journal of Herpetology*, 48(3), 394–406.
- Portillo, F., & Greenbaum, E. (2014b). At the edge of a species boundary: A new and relatively young species of *Leptopelis* (Anura: Arthroleptidae) from the Itombwe Plateau. *Democratic Republic of the Congo. Herpetologica*, 70(1), 100–119. <https://doi.org/10.1655/HERPETOLOGICA-D-12-00087>
- Pritchard, J. K., Wen, W., & Falush, D. (2003). *Documentation for the structure software, version 2*. University of Chicago, Chicago.
- Raven Pro. Pro Interactive Sound Analysis Software (Version 1.4) [Computer software]. Ithaca, NY: The Cornell Lab of Ornithology. <http://ravensoundsoftware.com/>
- Rambaut, A., Drummond, A. J., Xie, D., Baele, G., & Suchard, M. A. (2018). Posterior summarization in Bayesian phylogenetics using Tracer 1.7. *Systematic Biology*, 67(5), 901–904. <https://doi.org/10.1093/sysbio/syy032>
- Rochette, N. C., Rivera-Colón, A. G., & Catchen, J. M. (2019). Stacks 2: Analytical methods for paired-end sequencing improve RADseq-based population genomics. *Molecular Ecology*, 28(21), 4737–4754. <https://doi.org/10.1111/mec.15253>
- Rödel, M.-O., Emmrich, M., Penner, J., Schmitz, A., & Barej, M. F. (2014). The taxonomic status of two West African *Leptopelis* species: *L. macrotis* Schiøtz, 1967 and *L. spiritusnoctis* Rödel, 2007 (Amphibia: Anura: Arthroleptidae). *Zoosystematics and Evolution*, 90, 21–31. <https://doi.org/10.3897/zse.90.7120>
- Ryan, P. G., Bloomer, P., Moloney, C. L., Grant, T. J., & Delpont, W. (2007). Ecological speciation in south Atlantic island finches. *Science*, 315, 1420–1423. <https://doi.org/10.1126/science.1138829>
- Salzmann, U., & Hoelzmann, P. (2005). The Dahomey gap: an abrupt climatically induced rain forest fragmentation in West Africa during the late Holocene. *The Holocene*, 15(2), 190–199. <https://doi.org/10.1191/0959683605hl799rp>
- Sánchez-Vialas, A., Calvo-Revuelta, M., Castroviejo-Fisher, S., & De la Riva, I. (2020). Synopsis of the Amphibians of Equatorial Guinea based upon the authors' field work and Spanish natural history collections. *Proceedings of the California Academy of Sciences*, 66(8), 137–230.
- Schiøtz, A. (1967). The treefrogs (Rhacophoridae) of West Africa. *Spolia Zoologica Musei Haunienses*, 25, 1–346.
- Schiøtz, A. (1999). *Treefrogs of Africa*. Edition Chimaira.
- Schluter, D. (2009). Evidence for ecological speciation and its alternative. *Science*, 323, 737–741. <https://doi.org/10.1126/science.1160006>
- Springer, M. S., Meredith, R. W., Gatesy, J., Emerling, C. A., Park, J., Rabosky, D. L., Stadler, T., Steiner, C., Ryder, O. A., Janečka, J. E., Fisher, C. A., & Murphy, W. J. (2012). Macroevolutionary dynamics and historical biogeography of primate diversification inferred from a species supermatrix. *PLoS One*, 7, e49521. <https://doi.org/10.1371/journal.pone.0049521>
- Streicher, J. W., Devitt, T. J., Goldberg, C. S., Malone, J. H., Blackmon, H., & Fujita, M. K. (2014). Diversification and asymmetrical gene flow across time and space: lineage sorting and hybridization in polytypic barking frogs. *Molecular Ecology*, 23(13), 3273–3291. <https://doi.org/10.1111/mec.12814>
- Thuiller, W., Georges, D., Engler, R., & Breiner, F. (2016). Package 'biomod2': Species distribution modeling within an ensemble forecasting framework. R package version 3.3-7.
- Tolley, K. A., Townsend, T. M., & Vences, M. (2013). Large-scale phylogeny of chameleons suggests African origins and Eocene diversification. *Proceedings of the Royal Society B: Biological Sciences*, 280, 20130184.
- Trauth, M. H., Larrasoña, J. C., & Mudelsee, M. (2009). Trends, rhythms, and events in Plio-Pleistocene African climate. *Quaternary Science Reviews*, 28(5–6), 399–411. <https://doi.org/10.1016/j.quascirev.2008.11.003>
- Uy, J. A. C., & Borgia, G. (2000). Sexual selection drives rapid divergence in bowerbird display traits. *Evolution*, 54(1), 273–278. <https://doi.org/10.1111/j.0014-3820.2000.tb00027.x>
- van Proosdij, A. S. J., Sosef, M. S. M., Wieringa, J. J., & Raes, N. (2016). Minimum required number of specimen records to develop accurate species distribution models. *Ecography*, 39, 542–552. <https://doi.org/10.1111/ecog.01509>
- Warren, D. L., Matzke, N., Cardillo, M., Baumgartner, J., Beaumont, L., Huron, N., & Dinnage, R. (2019). ENMTools (Software Package). URL: <https://github.com/danlwarren/ENMTools>. doi:<https://doi.org/10.5281/zenodo.3268814>
- Wickham, H. (2016). *ggplot2: Elegant Graphics for Data Analysis*. Springer-Verlag. <https://ggplot2.tidyverse.org>
- Wiens, J. J. (2004). Speciation and ecology revisited: Phylogenetic niche conservatism and the origin of species. *Evolution*, 58(1), 193–197. <https://doi.org/10.1111/j.0014-3820.2004.tb01586.x>
- Wilson, A. C., Maxson, L. R., & Sarich, V. M. (1974). Two types of molecular evolution. Evidence from studies of interspecific hybridization. *Proceedings of the National Academy of Sciences*, 71(7), 2843–2847.
- Xu, M., & Shaw, K. L. (2020). Spatial mixing between calling males of two closely related, sympatric crickets suggests beneficial heterospecific interactions in a nonadaptive radiation. *Journal of Heredity*, 111(1), 84–91.
- Zhen, Y., Harrigan, R. J., Ruegg, K. C., Anderson, E. C., Ng, T. C., Lao, S., & Smith, T. B. (2017). Genomic divergence across ecological gradients in the Central African rainforest songbird (*Andropadus virens*). *Molecular Ecology*, 26(19), 4966–4977.

SUPPORTING INFORMATION

Additional supporting information may be found in the online version of the article at the publisher's website.

How to cite this article: Jaynes, K. E., Myers, E. A., Gvoždík, V., Blackburn, D. C., Portik, D. M., Greenbaum, E., Jongsma, G. F. M., Rödel, M.-O., Badjedjea, G., Bamba-Kaya, A., Baptista, N. L., Akuboy, J. B., Ernst, R., Kouete, M. T., Kusamba, C., Masudi, F. M., McLaughlin, P. J., Nneji, L. M., Onadeko, A. B., ... Bell, R. C. (2021). Giant Tree Frog diversification in West and Central Africa: Isolation by physical barriers, climate, and reproductive traits. *Molecular Ecology*, 00, 1–20. <https://doi.org/10.1111/mec.16169>